Fluid-structure interaction with a staged algorithm

by Mario Storti, Norberto Nigro, Rodrigo Paz,

Lisandro Dalcín, Gustavo A. Ríos Rodríguez, Ezequiel López

Centro Internacional de Métodos Numéricos
en Ingeniería - CIMEC
INTEC, (CONICET-UNL), Santa Fe, Argentina
<mstorti@intec.unl.edu.ar>
http://www.cimec.org.ar/mstorti

(document-version "fsis-conf-0.0.2") (document-date "2006/12/10 15:47:48 UTC")

Multiphysics

- **Complex coupled problems involving many fields. Some coupling not *a priori* known.**
- **Interaction of acoustics with flexible structures.**
- **Magneto-Hydrodynamics devices**
- **Micro-Electro-Mechanical devices**
- **Thermo-Mechanical problems, like continuous casting.**
- **Fluid-Structure interaction (wing flutter, flow induced vibrations...).**

This article is concerned with the numerical integration of this type of problems when they are coupled in a *loose* or *strong* manner.

Monolithic vs. Partitioned

- **For simple structural problems with few vibrational degrees of freedom it is possible to combine the fluid and the structure in a single formulation. Then the full system can be integrated with a explicit or implicit scheme. These *"monolithic"* methods can be very robust but are in general not modular and parallel efficiency is difficult to reach.**
- **An efficient alternative is to solve each subproblem in a partitioned procedure where time and space discretization methods could be different. Such a scheme simplifies explicit/implicit integration and it is in favor of the use of different codes specialized on each sub-area. In this work a staggered fluid-structure coupling algorithm is considered.**

Basic (weakly coupled) partitioned FSI algorithm

- **(i) transfer the motion of the wet boundary of the solid to the fluid problem,**
- **(ii) update the position of the fluid boundary and the bulk fluid mesh accordingly,**
- **(iii) advance the fluid system and compute new pressures (and the stress field if it is necessary),**
- **(iv) convert the new fluid pressure (and stress field) into a structural load, and**
- **(v) advance the structural system under the flow loads.**

Staged (strongly coupled) partitioned FSI algorithm

States: $\mathbf{u}$ structure, $\mathbf{w}$ fluid, $\mathbf{X}$ mesh.

Initialize variables:
for $n = 0$ **to** n_{step} **do** {**Main time step loop**}
  $t^n = n\Delta t$,
  $\mathbf{X}^n = \mathrm{CMD}(\mathbf{u}^n)$ {**run CMD code**}
  $\mathbf{u}^{(n+1)P} = \mathbf{u}^{(n+1,0)} = \mathrm{predictor}(\mathbf{u}^n, \mathbf{u}^{n-1})$ { **compute predictor** }
  for $i = 0$ **to** n_{stage} **do** {**stage loop**}
    $\mathbf{X}^{n+1,i+1} = \mathrm{CMD}(\mathbf{u}^{n+1,i})$
    $\mathbf{w}^{n+1,i+1} = \mathrm{CFD}(\mathbf{w}^n, \mathbf{X}^{n+1,i+1}, \mathbf{X}^n)$ {**Fluid solver CFD**}
    compute structural loads $(\mathbf{w}^n, \mathbf{w}^{n+1,i+1})$
    $\mathbf{u}^{n+1,i+1} = \mathrm{CSD}(\mathbf{u}^n, \mathbf{w}^n, \mathbf{w}^{n+1,i+1})$ {**Structure solver CSD**}
  end for
end for

Stability, weak vs. strong (staged)

- **Stage loop is a fixed point iteration to the monolithic (strong coupled) integration, so that if the stage loop is iterated and converged the algorithm has the stability properties of the monolithic one. ($\Delta t_{\rm crit,staged} \gg \Delta t_{\rm crit,weak}$)**
- **However, time step may be limited by convergence of the stage loop, i.e. it may happen that for a given Δt the fixed point stage loop does not converge.**
- **Computational cost is increased by the number of *stages*.**

This is an ongoing research. So far, we have no analytic results about stability (estimations for critical time step). [Storti M.; Nigro N.; Paz, R.R. "Strong coupling strategy for fluid structure interaction problems in supersonic regime via fixed point iteration" *Journal of Sound and Vibration* (2006, submitted, available at `http://www.cimec.org.ar/mstorti`).]

ALE invariance

A key point in fluid-structure interaction problems is the use of the *"Arbitrary Lagrangian Eulerian formulation"* (ALE) , which allows the use of moving meshes. As the ALE convective terms affect the advective terms, some modifications are needed to the standard stabilization terms in order to get the correct amount of stabilization. Also boundary conditions at walls (slip or non-slip) and absorbing boundary conditions must be modified when ALE is used.

ALE invariance (cont.)

- **Discrete equations are not invariant under an arbitrary Galilean transformation, mainly because the importance of the advective terms are relative to the frame of reference.**
- **For instance, a fluid which is at rest in frame S does not need stabilization, whereas in a frame S' with relative velocity $\mathbf{v}$ it may have a high Pèclet number and then it will need stabilization.**
- **However, when using ALE formulations with moving domains, stabilization is based on the velocity of the *fluid relative to the mesh*. With this additional degree of freedom introduced with moving meshes a physical problem can be posed in different Galilean frames and in such a way that the velocity of the fluid *relative to the mesh is the same*. Then the question can be posed of whether discrete stabilized equations give the same solution (after appropriate transformation laws) in these equivalent situations. If the scheme is not invariant then great chances exist that the scheme adds more diffusion in one frame than in other, and then to be unstable or too diffusive. If the discrete formulation pass the test we say that it is *"ALE invariant"*.**

ALE invariance test case. Sudden stop of gas container

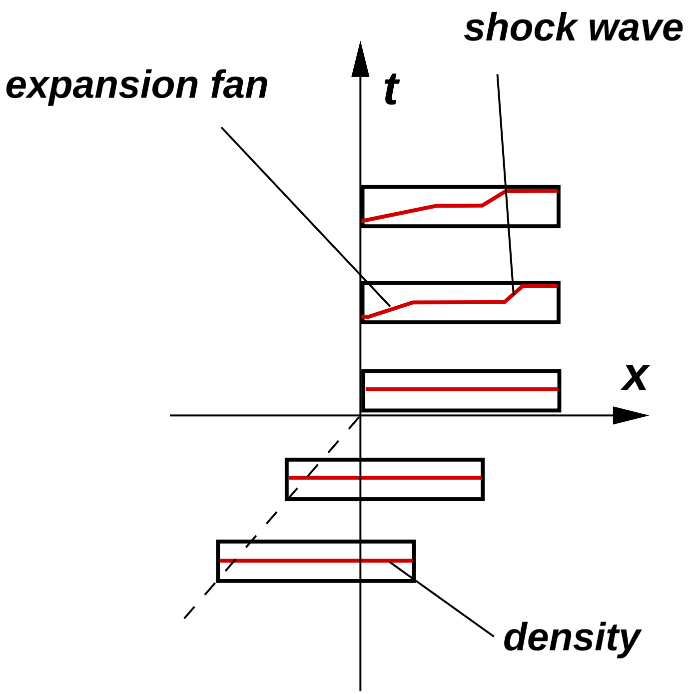

container initially moving at constant speed u0 is suddenly stopped

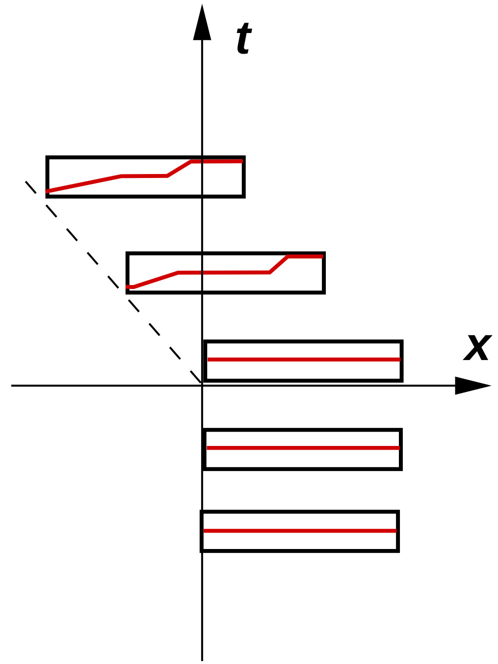

container initially at rest is suddenly put in movement with constant negative speed −u0

ALE invariance. SUPG Stabilization term

$$\frac{\partial ! U_c}{\partial t} + \frac{\partial \mathcal{F}_{c,x}}{\partial x} = \frac{\partial \mathcal{F}_{d,x}}{\partial x}; \qquad \textbf{(gov. eqs. in cons. form)}$$

$$C\frac{\partial \mathbf{U}}{\partial t} + \mathbf{A}\frac{\partial \mathbf{U}}{\partial x} = \mathbf{K}\frac{\partial^2 \mathbf{U}}{\partial x^2}; \quad \textbf{(gov. eqs. in quasi-linear form)} \qquad (1)$$

Sufficient conditions for ALE invariance ($!\tilde{A} = \mathbf{A} - \mathbf{v}_{\mathrm{mesh}}\mathbf{C}$)

$$P = \nabla N \cdot !\tilde{A}\boldsymbol{\tau}\mathbf{C}^{-1}; \quad \textbf{(SUPG pert. function)}$$

$$\boldsymbol{\tau} \ \textbf{ transform as } \mathbf{U}\times\mathbf{U}, \quad \left(\textbf{i.e. } \boldsymbol{\tau}' = \frac{\partial \mathbf{U}'}{\partial \mathbf{U}}\boldsymbol{\tau}\frac{\partial \mathbf{U}}{\partial \mathbf{U}'}\right). \qquad (2)$$

This last is verified if $\boldsymbol{\tau}$ is $f(\mathbf{C}^{-1}!\tilde{A})$, for instance (inviscid case):

$$\boldsymbol{\tau} = \frac{h}{\max|\lambda_j|}\mathbf{I}, \ \ \lambda_j = \mathrm{eig}(\mathbf{C}^{-1}!\tilde{A}), \qquad \textbf{(max. eigenv.)}$$

$$\boldsymbol{\tau} = h|\mathbf{C}^{-1}!\tilde{A}|^{-1}. \qquad \textbf{(} | \cdot | \textbf{ in matrix sense)} \qquad (3)$$

ALE invariance. Sudden stop of a gas container

$\gamma = 1.4$, $u_0/c_0 = 0.5$. **Results in both reference systems are equivalent to machine precision.**

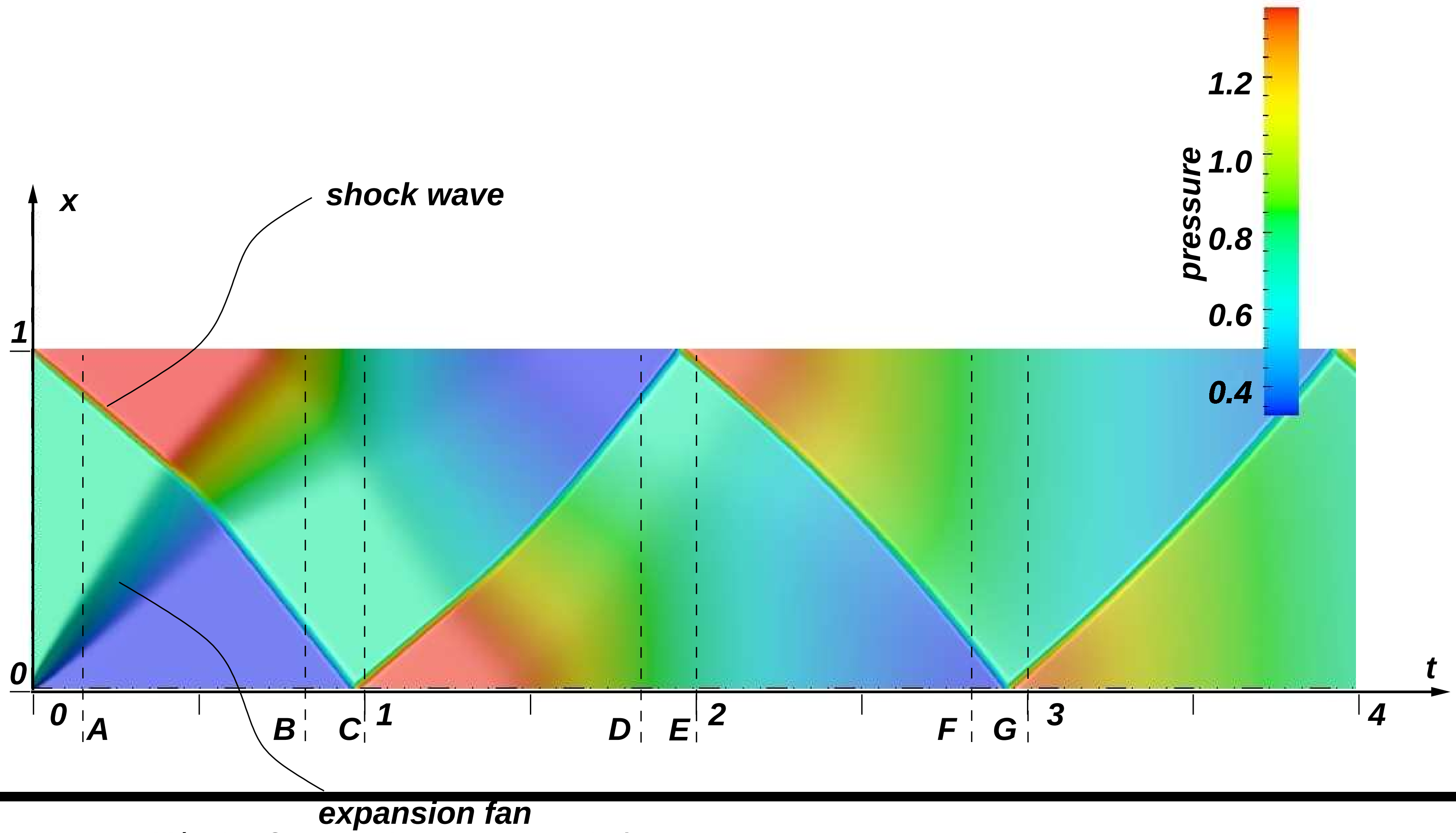

ALE invariance. Sudden stop of a gas container (cont.)

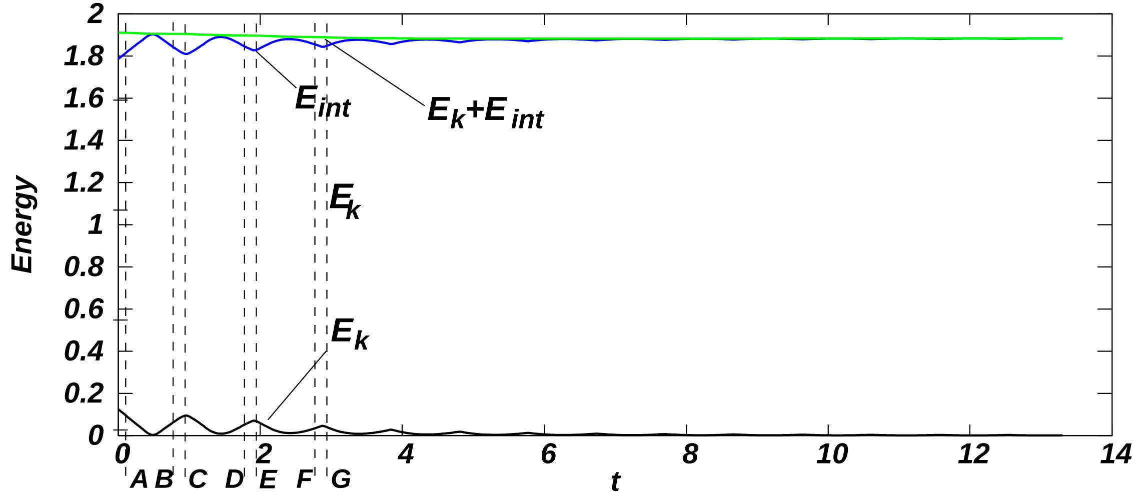

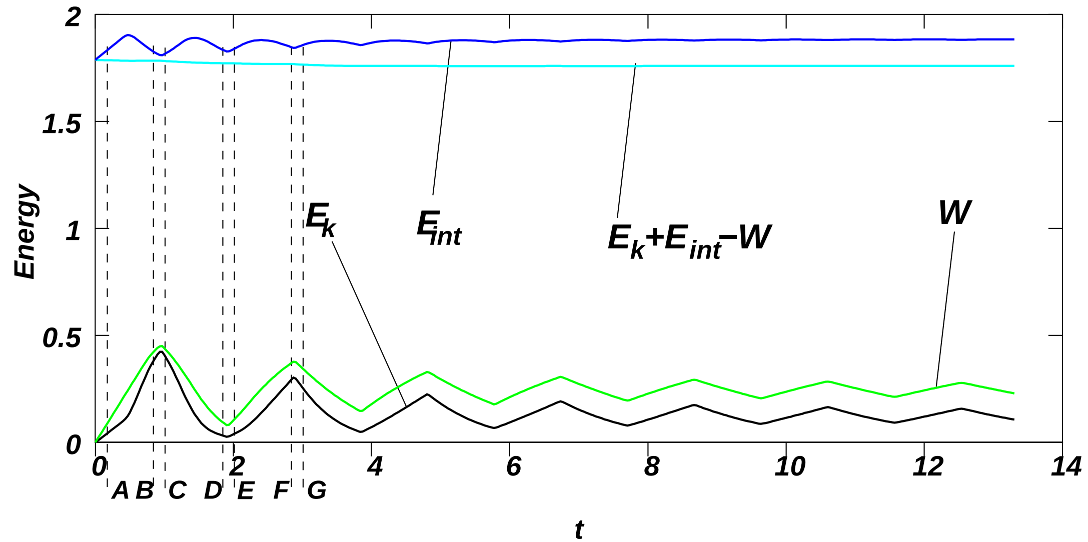

(Up) Energy balance in reference system fixed w.r.t container)
(Down) Energy balance in reference system fixed w.r.t initial gas at rest)

Boundary conditions for advective diffusive systems

Well known theory and practice for advective systems say that at a boundary *the number of Dirichlet conditions should be equal to the number of incoming characteristics*.

$$\frac{\partial \mathbf{U}}{\partial t} + \frac{\partial \mathcal{F}_{c,j}(\mathbf{U})}{\partial x_j} = 0$$

$$A_{c,j} = \frac{\partial \mathcal{F}_{c,j}(\mathbf{U})}{\partial \mathbf{U}}, \qquad \textbf{advective Jacobian}$$

Nbr. of incoming characteristics $= \mathrm{sum}(\mathrm{eig}(\mathbf{A} \cdot \hat{\mathbf{n}}) < 0)$

$\hat{\mathrm{n}}$ **is the exterior normal.**

Adding extra Dirichlet conditions leads to spurious shocks, and lack of a Dirichlet conditions leads to instability.

Boundary conditions for advective diffusive systems (cont.)

For simple scalar advection problems the Jacobian is the transport velocity. The rule is then to check the projection of velocity onto the exterior normal.

For more complex flows (i.e. with *non diagonalizable Jacobians*, as gas dynamics or shallow water eqs.) the number of incoming characteristics may be approx. predicted from the flow conditions.

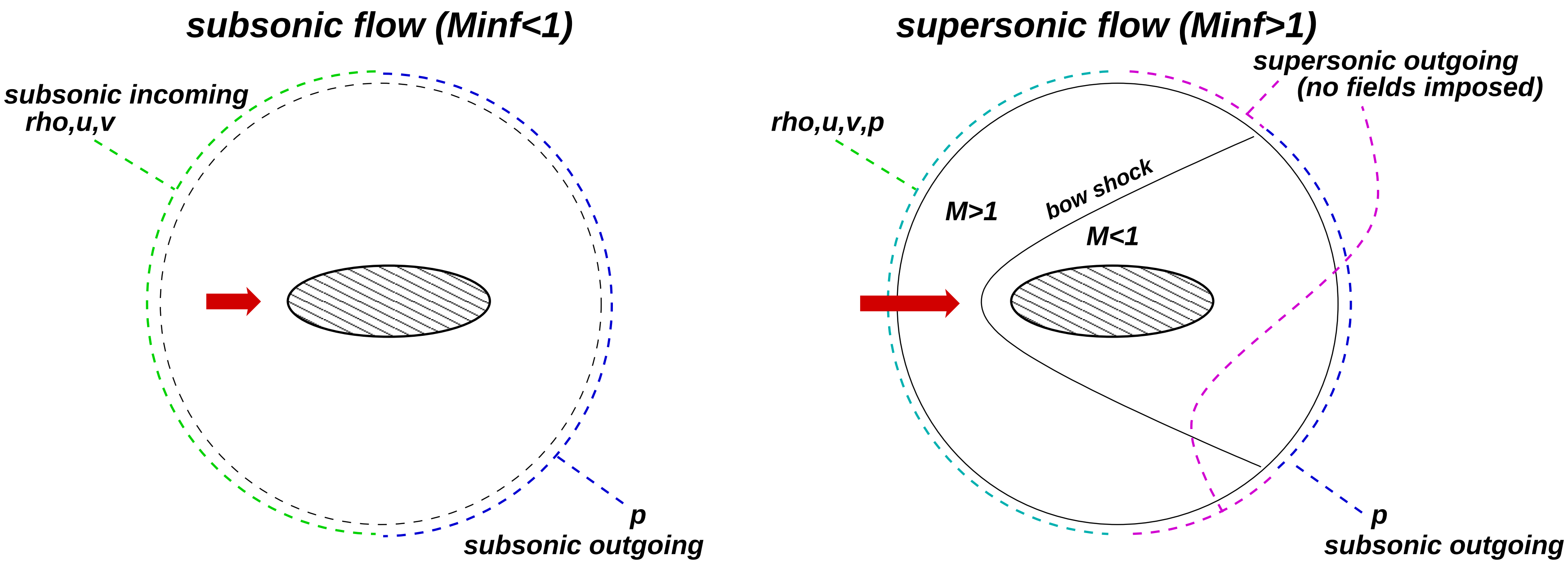

Absorbing boundary conditions

However, this kind of conditions are, generally, *reflective*. First order absorbing boundary conditions may be constructed by imposing exactly the components along the incoming characteristics.

$$\mathbf{\Pi}^-(\mathbf{U}_{\rm ref})\,(\mathbf{U}-\mathbf{U}_{\rm ref}) = 0.$$

$\mathbf{\Pi}^-$ is the projection operator onto incoming characteristics. It can be obtained straightforwardly from the projected Jacobian.

This assumes linearization of the equations around a state $\mathrm{U}_{\rm ref}$. For linear problems $\mathbf{A}_{c,j}$ do not depend on U, and then neither the projection operator, so that absorbing boundary conditions coefficients are constant.

Absorbing boundary conditions (cont.)

For non-linear problems the Jacobian and projection operator may vary and then the above mentioned b.c.'s are not fully absorbing.

In some cases the concept of characteristic component may be extended to the non-linear case: the *"Riemann invariants"*. Fully absorbing boundary conditions could be written in terms of the invariants:

$$w_j = w_{\mathrm{ref},j}, \quad \text{if } w_j \text{ is an incoming R.I.}$$

- **R.I. are computed analytically. There are no automatic (numerical) techniques to compute them. (They amount to compute an integral in phase space *along a specific path*).**
- **R.I. are known for shallow water, channel flow (for rectangular and triangular channel shape). For gas dynamics the well known R.I. in fact are invariants only under isentropic conditions (i.e. not truly invariant).**

Absorbing boundary conditions (cont.)

Search for an absorbing boundary condition that

- **should be fully absorbent in non-linear conditions, and**
- **can be computed numerically (no need of analytic expressions like R.I.)**

Solution: ***Use last state as reference state, ULSAR*****.**

$\mathbf{U}_{\rm ref} = \mathbf{U}^n$, $n =$ **time step number.**

$$\mathbf{\Pi}^{-}(\mathbf{U}^n)\,(\mathbf{U}^{n+1} - \mathbf{U}^n) = 0.$$

As $\mathbf{U}^{n+1} - \mathbf{U}^n$ is usually small, linearization is valid.

Absorbing boundary conditions (cont.)

Disadvantage: **Flow conditions are only determined from the initial state!! No external information comes from the outside.**

Solution: use a combination of linear/R.I. b.c.'s on incoming boundaries and use fully non-linear a.b.c's with previous state as reference state at the outlet.

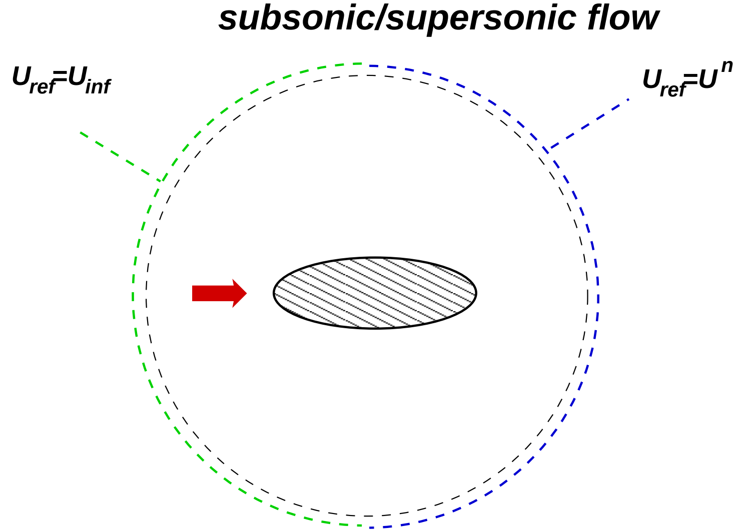

[Storti M.; Nigro N.; Paz, R.R. "Dynamic boundary conditions in Computational Fluid Dynamics" ***Journal of Computational Physics*** **(2006, submitted, available at `http://www.cimec.org.ar/mstorti`).]**

Stability of staged scheme.

Test case: elastically coupled gas container.

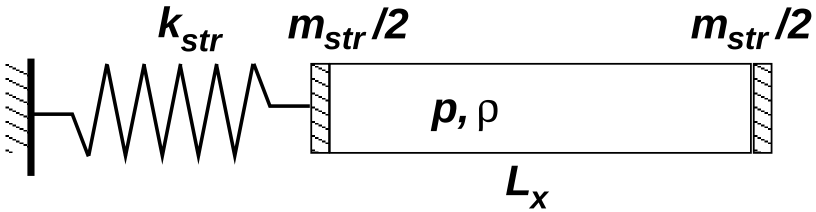

- $m_{\rm str}/(\rho L_x)$, **solid/fluid mass ratio,**
- $T_{\rm str}/T_{\rm acoust}$, **structure/acoustic time ratio,**
- $T_{\rm acoust}/T_{\rm visc}$, **acoustic/viscous time ratio,**

where

- $T_{\rm str} = 2\pi/\omega_{\rm str}$, $\omega_{\rm str} = \sqrt{k_{\rm str}/m_{\rm str}}$, **is the characteristic time of the structure, and**
- $T_{\rm acoust} = L_x/c_0$, $c_0 = \sqrt{\gamma p_0/\rho_0}$, **is the characteristic time for the fluid, i.e. the time needed for the sound speed to travel the length of the container,**
- $T_{\rm visc} = L_x^2/\nu$, **where** ν **is the kinematic viscosity.**

Stability of staged scheme. (cont.)

Colormap shows density vs. (x, t)**.**
Params: $L_x = 1$**, length of gas domain,** $N_x = 200$**, number of finite elements,** $\rho_0 = 1$**, density of gas,** $p_0 = 0.71429$**, density of gas,** $\gamma = 1.4$**, adiabatic index,** $\nu = 10^{-4}$**, kinematic viscosity of gas,** $\Delta t c_0/h = 0.5$**, Courant number (nondimensional time step),** $m_{\rm str} = 1$**, mass of container,** $k_{\rm str} = 200$**, spring constant. Initial displaceement** $x(0) = -0.1\, L_x$**.**

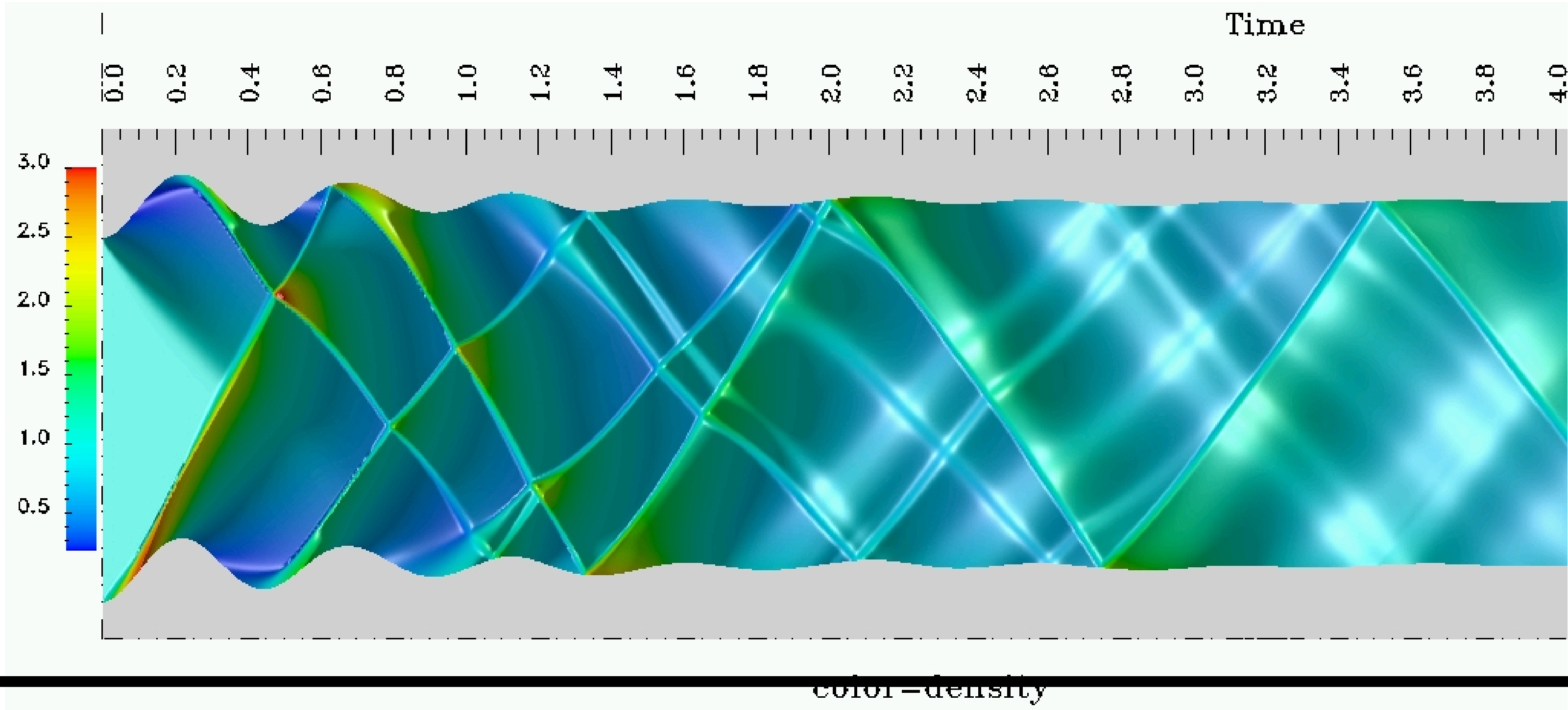

Influence of compressibility, viscosity, and structure

A series of experiments have been conducted in order to determine the stability of the algorithm, and the influence of several physical parameters.

- **If the compressibility of the fluid is high, i.e. $T_{\rm str}/T_{\rm acoust} \sim c_0$ small, then as the container walls compress the fluid a smaller amount of fluid is swept, and the added mass is lower, but the fluid has a certain additional stiffness. Experiments show that compressibility is destabilizing. In all cases stability can be recovered by increasing $n_{\rm stage}$ to 2.**
- **Even low viscosities can have a strong stabilizing effect since when instabilities are produced they have a very short wavelength and viscosity tends to be a prevailing effect for them.**
- **Scaling down $k_{\rm str}, m_{\rm str}$ keeps the characteristic time of the structure unchanged while increasing the force of the fluid onto the structure, and thus the gain of the tholw FSI interaction loop. This has then a strong destabilizing effect.**

Flutter of a flat solid plate

- **Viscous/inviscid supersonic flow (EULER/Compressible N-S eqs).**
- **Coupled through pressure and traction (viscous case only) on interface boundary.**

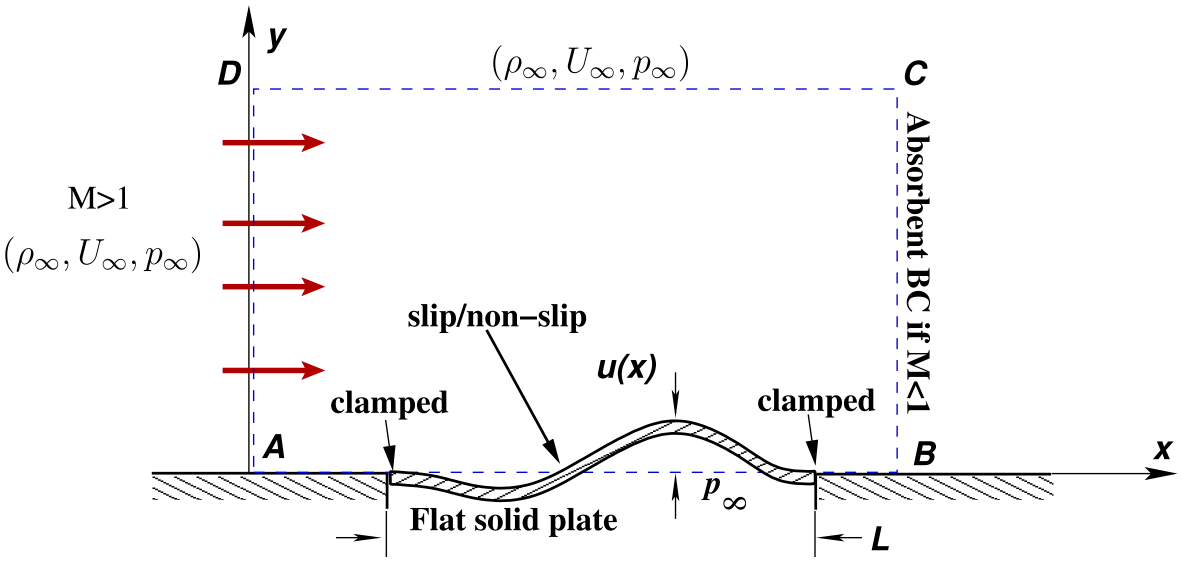

- **Thin plate theory for structure:** $m\ddot{u}(x,t) + D\frac{\partial^4 u(x,t)}{\partial x^4} = -(p - p_\infty) + f(x,t)$.
- **Undisturbed flow $(\rho, \mathbf{v}, p)_\infty$ is a solution of the problem for zero initial condition (solid problem).**

Analytical model based on Houbolt's approximation

- **Fluid Problem**

$$p - p_\infty = C_x \frac{\partial u}{\partial x} + C_t \frac{\partial u}{\partial t},$$

$$C_x = \frac{\rho_\infty {U_\infty}^2}{\sqrt{{\mathrm{M}_\infty}^2 - 1}}, \quad C_t = \frac{\rho_\infty U_\infty \left({\mathrm{M}_\infty}^2 - 2\right)}{({\mathrm{M}_\infty}^2 - 1)^{3/2}}.$$

- **Then, for the Plate Problem the deflection becomes**

$$m\ddot{u} + D\frac{\partial^4 u}{\partial x^4} = -C_x \frac{\partial u}{\partial x} - C_t \frac{\partial u}{\partial t}.$$

Analytical model based on Houbolt's approximation (cont.)

- **Using a global basis for displacements**

$$u(x) = \sum_{k=1}^{N} a_k \psi_k(x),$$

$$\psi_k(x) = \frac{4\,x(L-x)}{L^2}\,\sin(k\pi x/L).$$

- **The basis functions satisfy the essential boundary conditions for plate equation $u = (\partial u/\partial x) = 0$ at $x = 0, L$.**

Analytical model based on Houbolt's approximation (cont.)

- **Replacing $u(x)$ in the Houbolt's approximation and using Galerkin method**

$$\mathbf{M}\ddot{\mathbf{a}} + \mathbf{K}\mathbf{a} + \mathbf{H}_x\mathbf{a} + \mathbf{H}_t\dot{\mathbf{a}} = 0,$$

where

$$M_{jk} = \int_0^L m\,\psi_j(x)\,\psi_k(x)\,\mathrm{d}x,$$

$$K_{jk} = \int_0^L D\,\psi_j''(x)\,\psi_k''(x)\,\mathrm{d}x,$$

$$H_{x,jk} = \int_0^L C_x\,\psi_j(x)\,\psi_k'(x)\,\mathrm{d}x,$$

$$H_{t,jk} = \int_0^L C_t\,\psi_j(x)\,\psi_k(x)\,\mathrm{d}x.$$

Analytical model based on Houbolt's approximation (cont.)

- **If the ansatz $a(t) = \hat{\mathbf{a}}\mathbf{e}^{\lambda t}$ is proposed as a solution for the Plate Problem, the following eigenvalue problem is stated**

$$\left(\lambda^2\mathbf{M} + \lambda\mathbf{H}_t + \mathbf{K} + \mathbf{H}_x\right)\hat{\mathbf{a}} = 0.$$

- **Using time and mass non-dimensional parameters**

$$N_T = \left(\frac{T_{\text{fl}}}{T_{\text{str}}}\right)^2 = \frac{L/U_\infty}{\sqrt{mL^4/D}} = \frac{D}{mL^2{U_\infty}^2} \quad \textbf{and}$$

$$N_M = \frac{\rho_\infty L^3}{mL^2} = \frac{\rho_\infty L}{m},$$

the space of parameters is full covered.

Analytical model based on Houbolt's approximation (cont.)

- **Results for the Houbolt's model**
  - ▷ $N = 20$, $N_x = 5000$, **and a sweep in** M_∞ **while keeping constant** ρ_∞, m, L **and** D,

    i.e., $N_M = \mathrm{cte}$ **and** $N_T \propto {\mathrm{M}_\infty}^{-2}$.

Analytical model based on Houbolt's approximation (cont.)

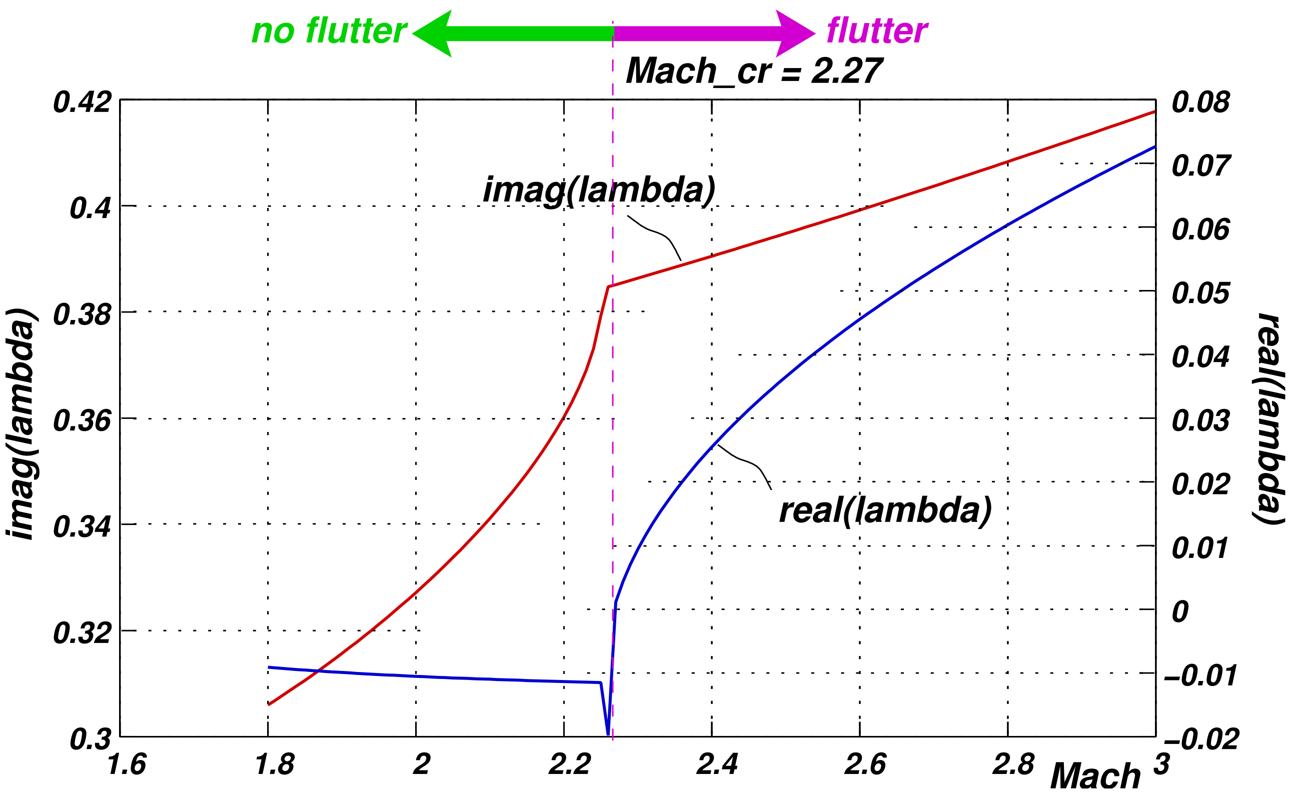

Flutter mode appears for $\mathrm{M}_\infty \geq 2.27$
or $N_T = 4.3438 \times 10^{-5}$ **and** $N_M = 0.055$.

Staged FSI-FEM Results for flutter

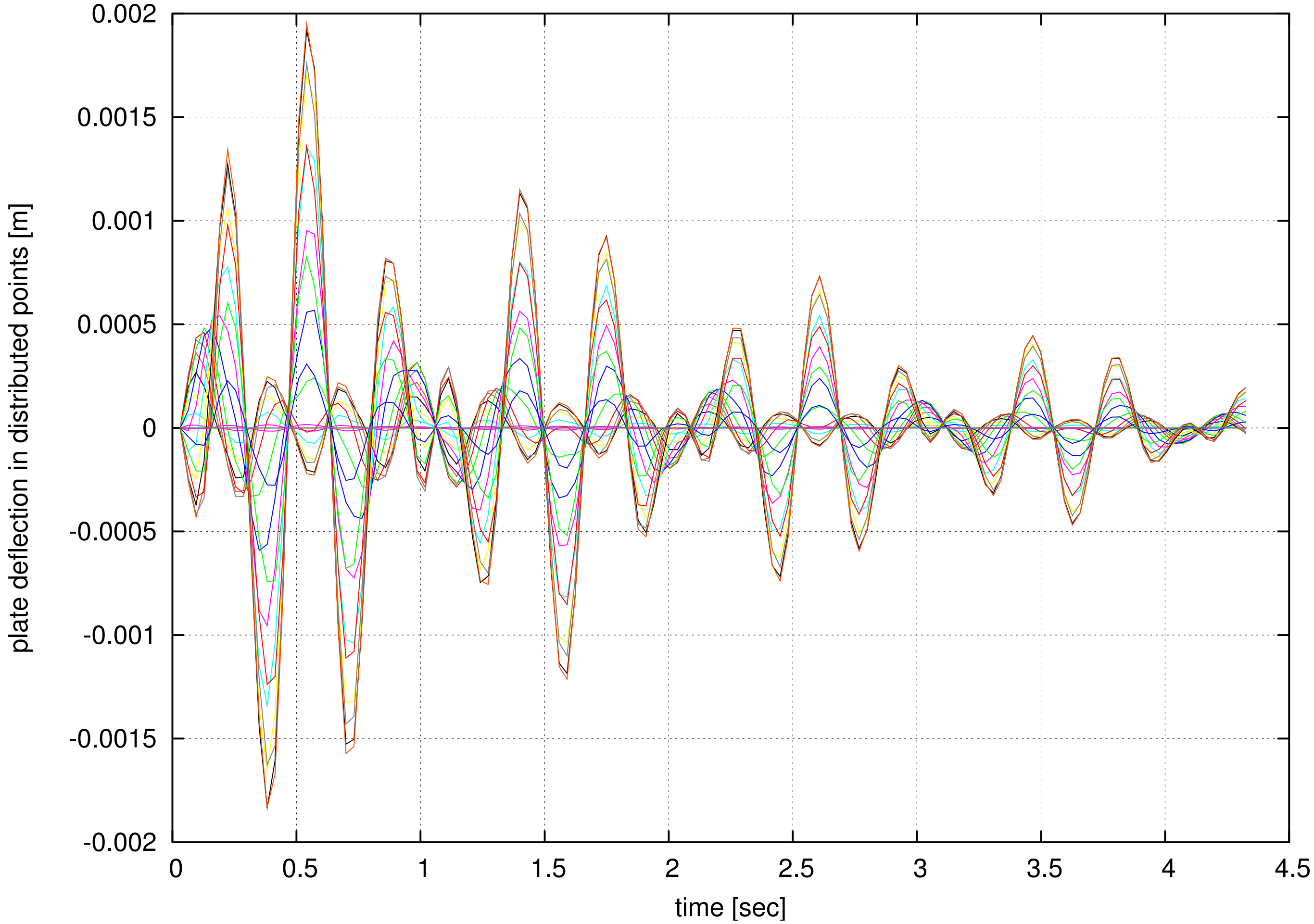

Structure response at M=1.8

Staged FSI-FEM Results for flutter (cont.)

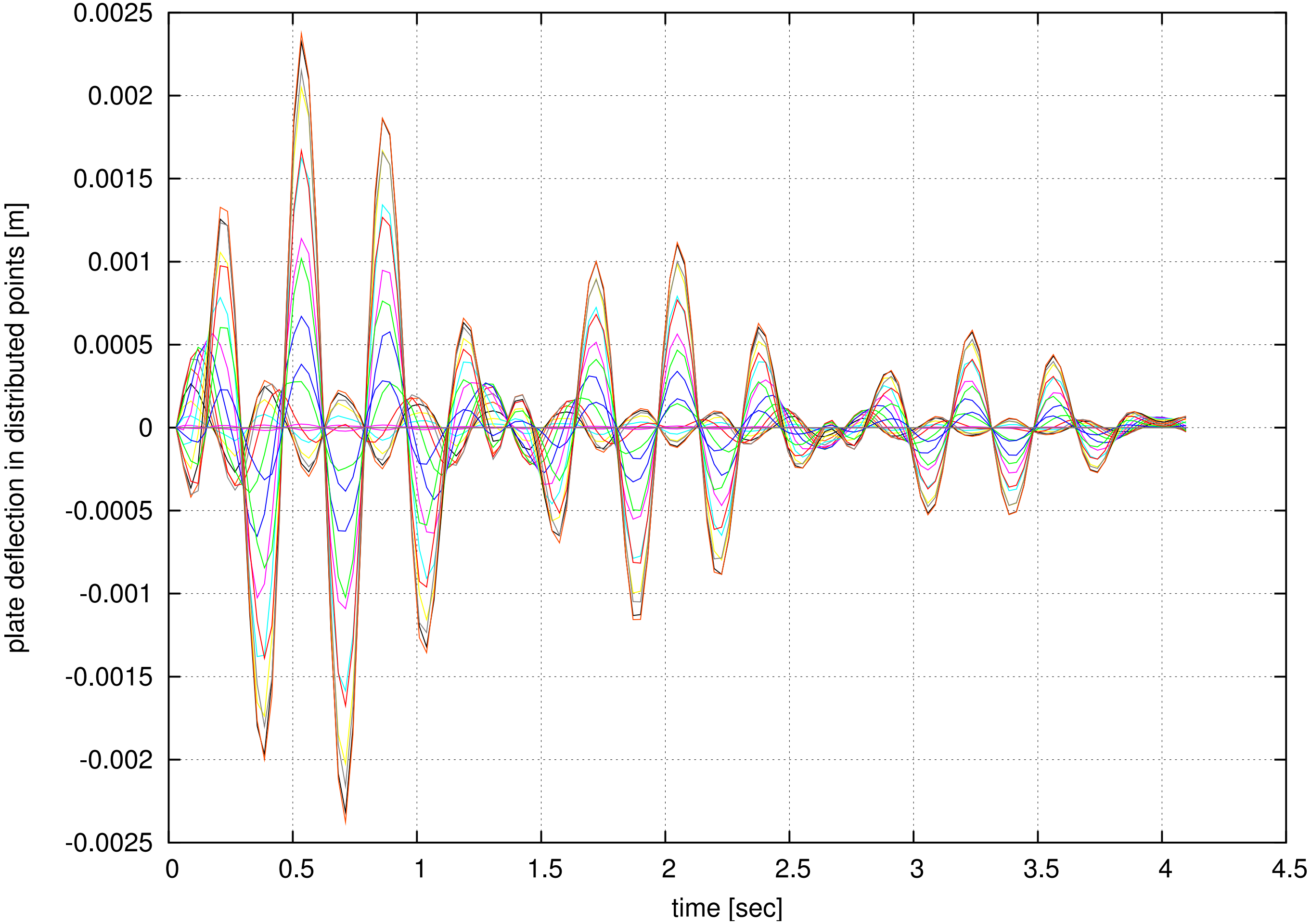

Structure response at M=2.0

Staged FSI-FEM Results for flutter (cont.)

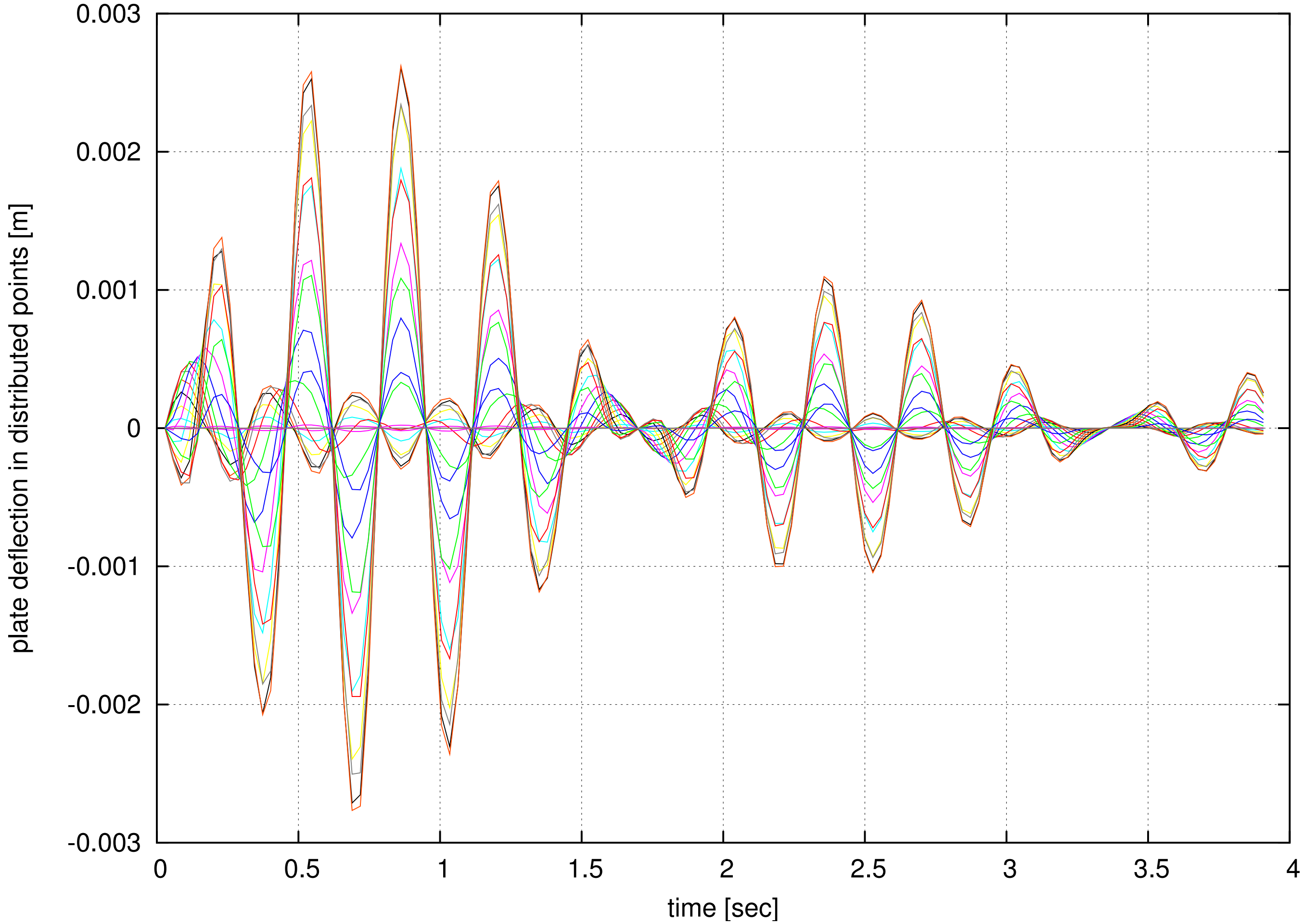

Structure response at M=2.1

Staged FSI-FEM Results for flutter (cont.)

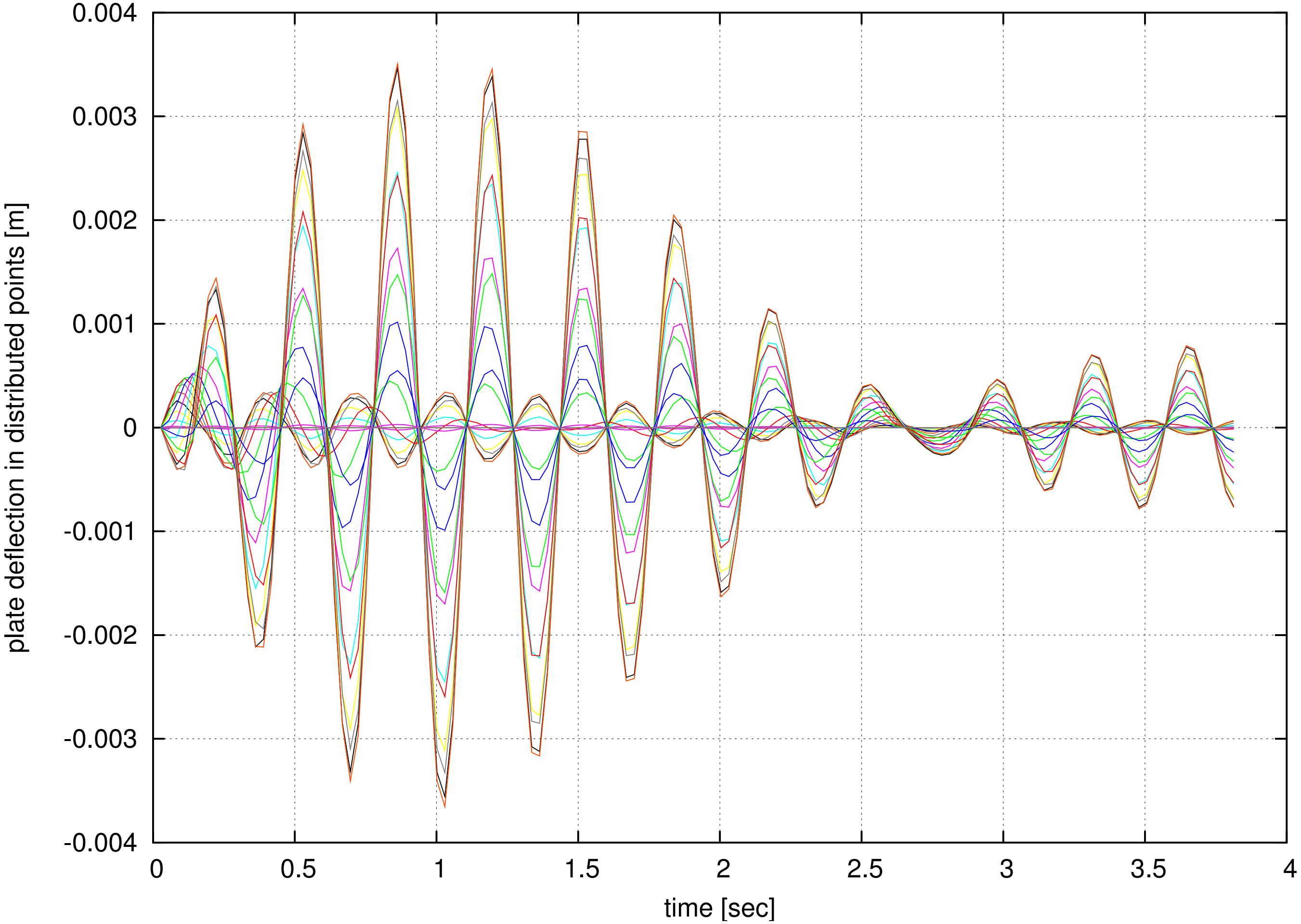

Structure response at M=2.2

Staged FSI-FEM Results for flutter (cont.)

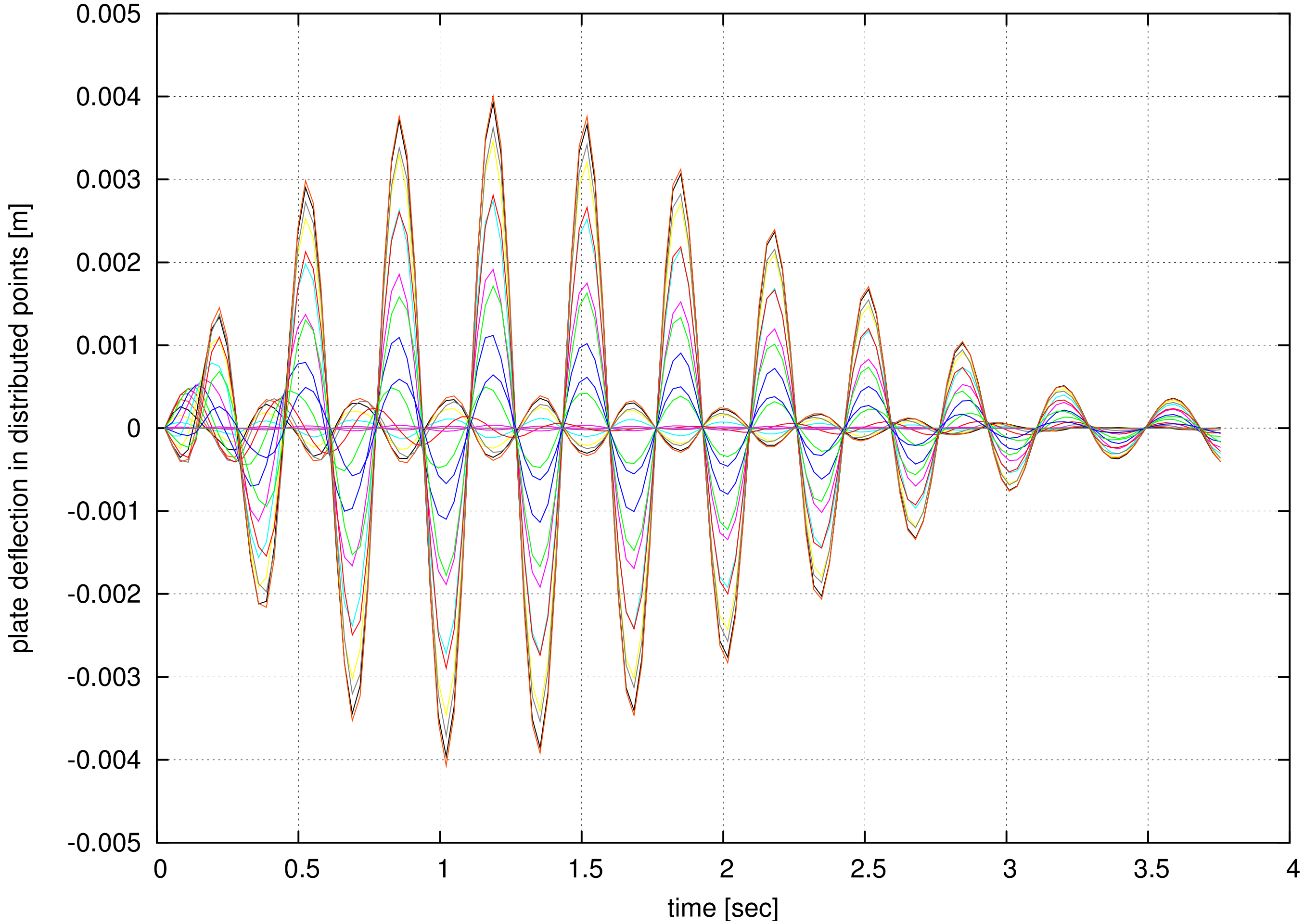

Structure response at M=2.225

Staged FSI-FEM Results for flutter (cont.)

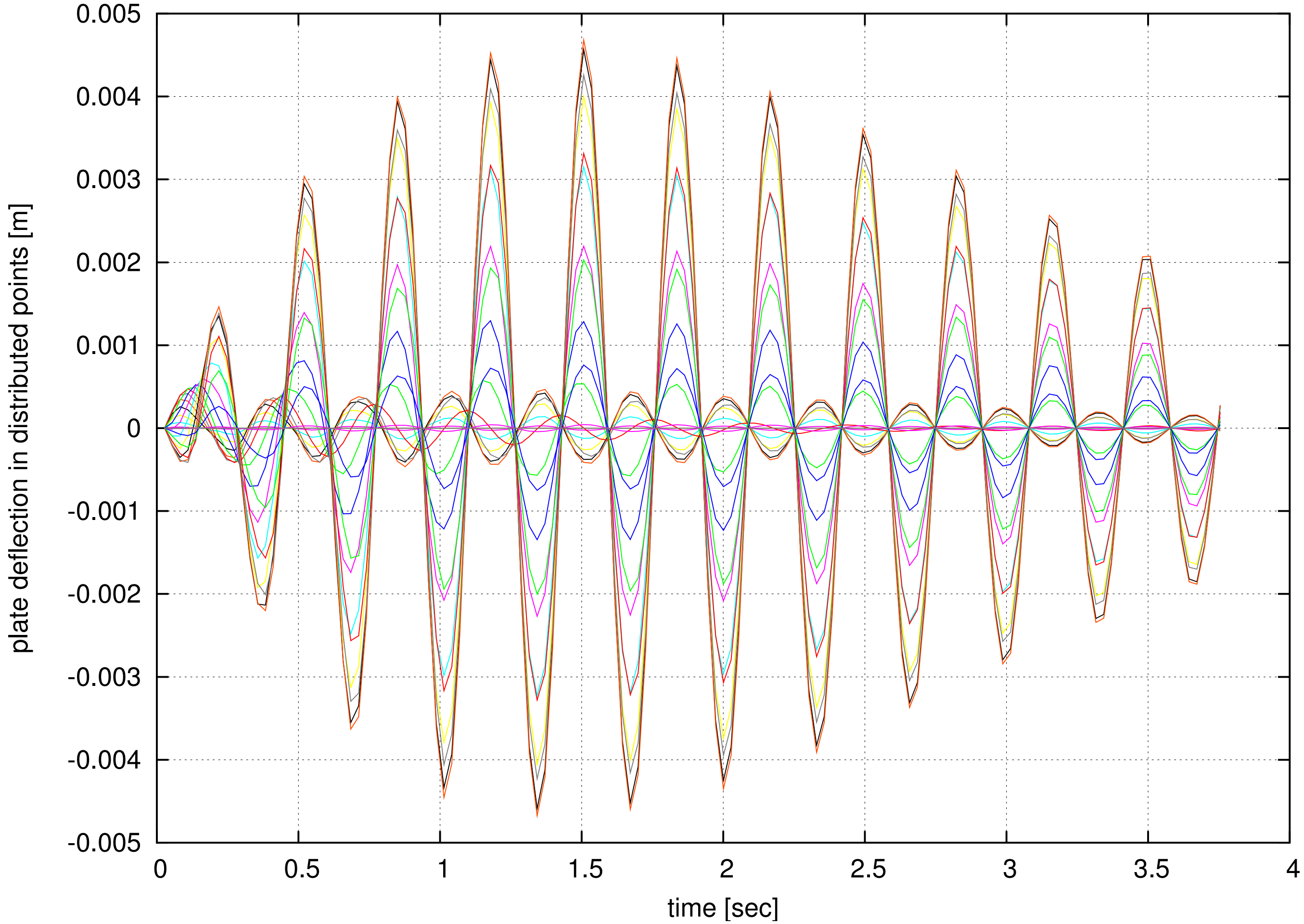

Structure response at M=2.25

Staged FSI-FEM Results for flutter (cont.)

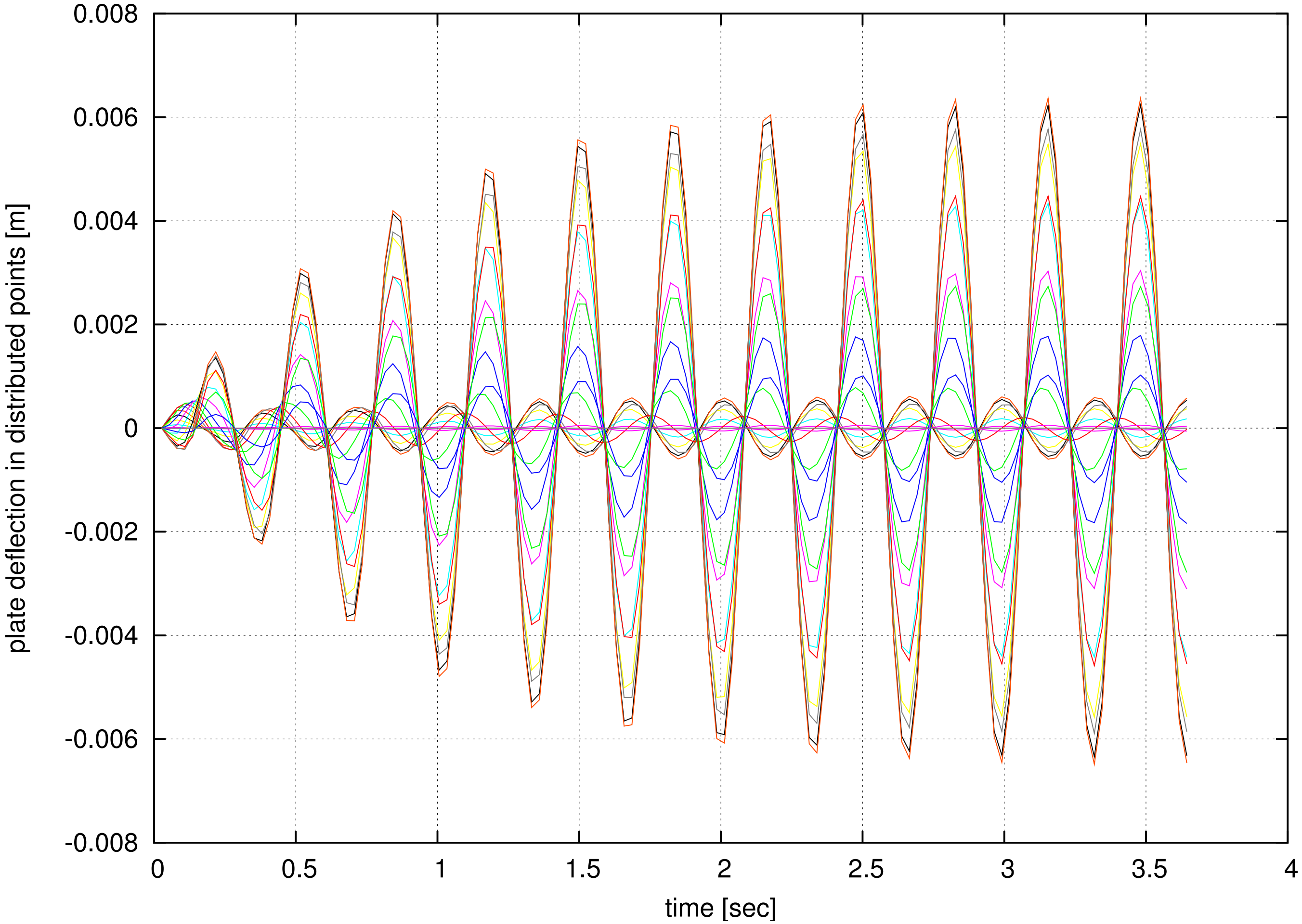

Structure response at M=2.275

Staged FSI-FEM Results for flutter (cont.)

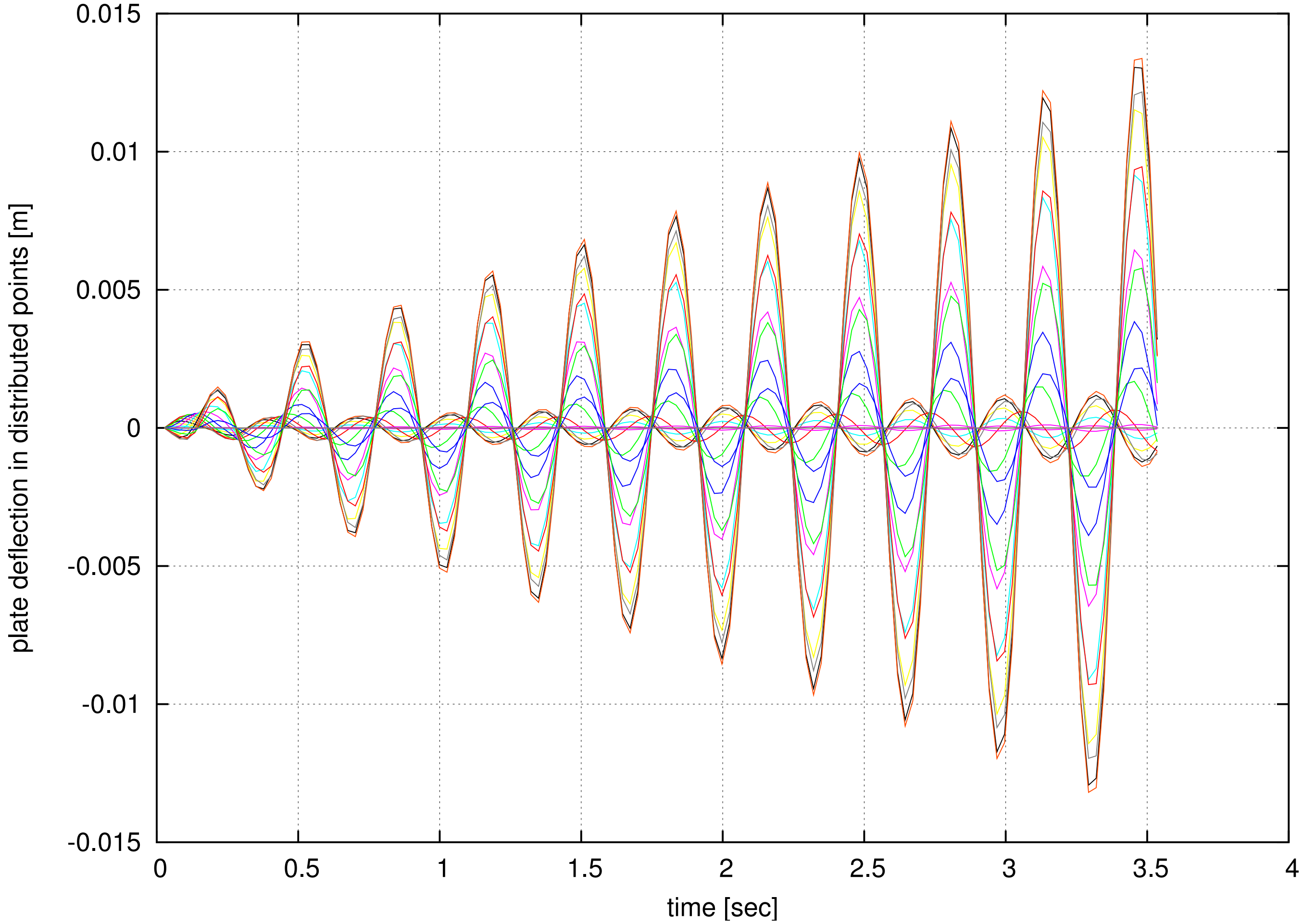

Structure response at M=2.3

Staged FSI-FEM Results for flutter (cont.)

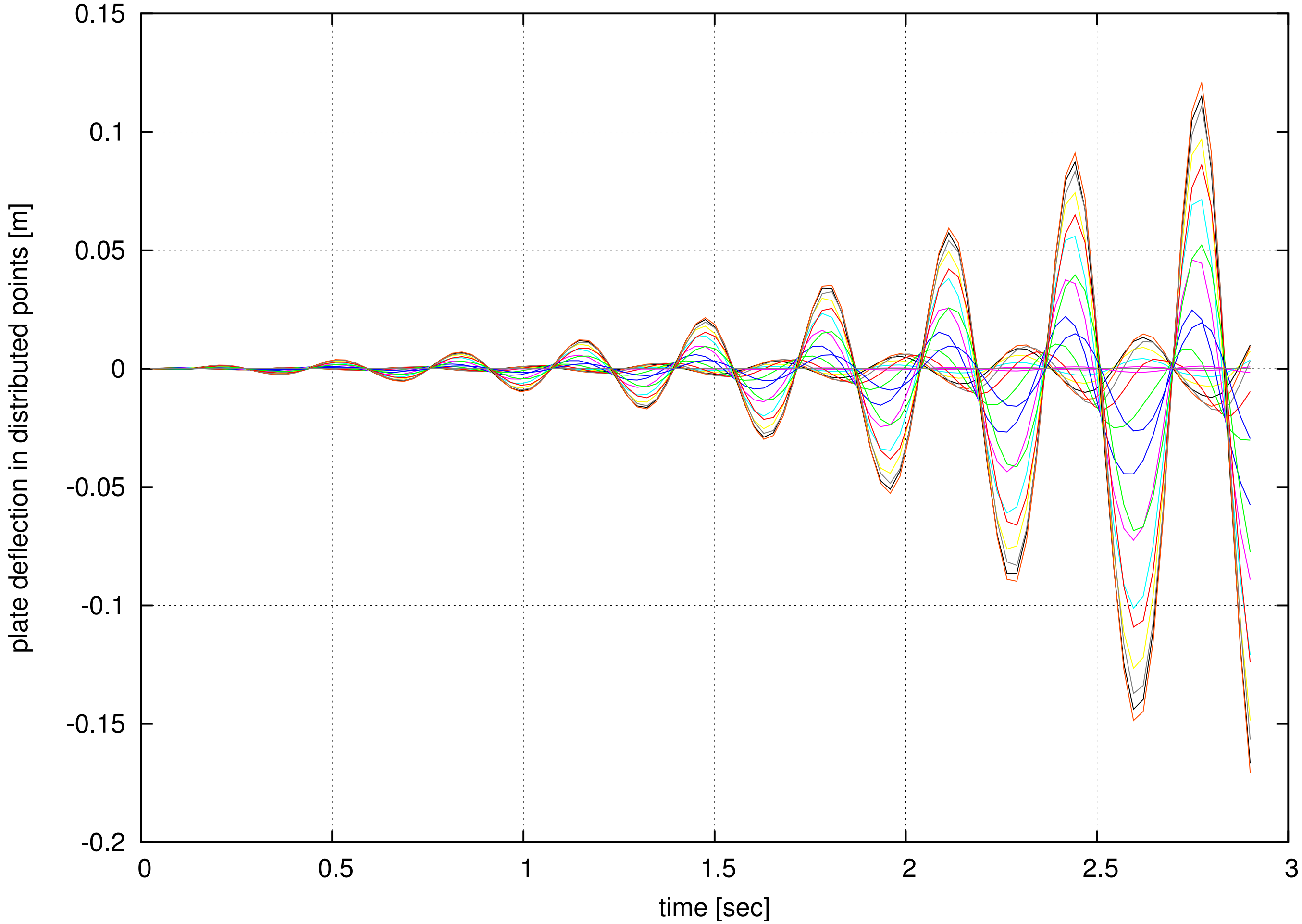

Structure response at M=2.5

Staged FSI-FEM Results for flutter (cont.)

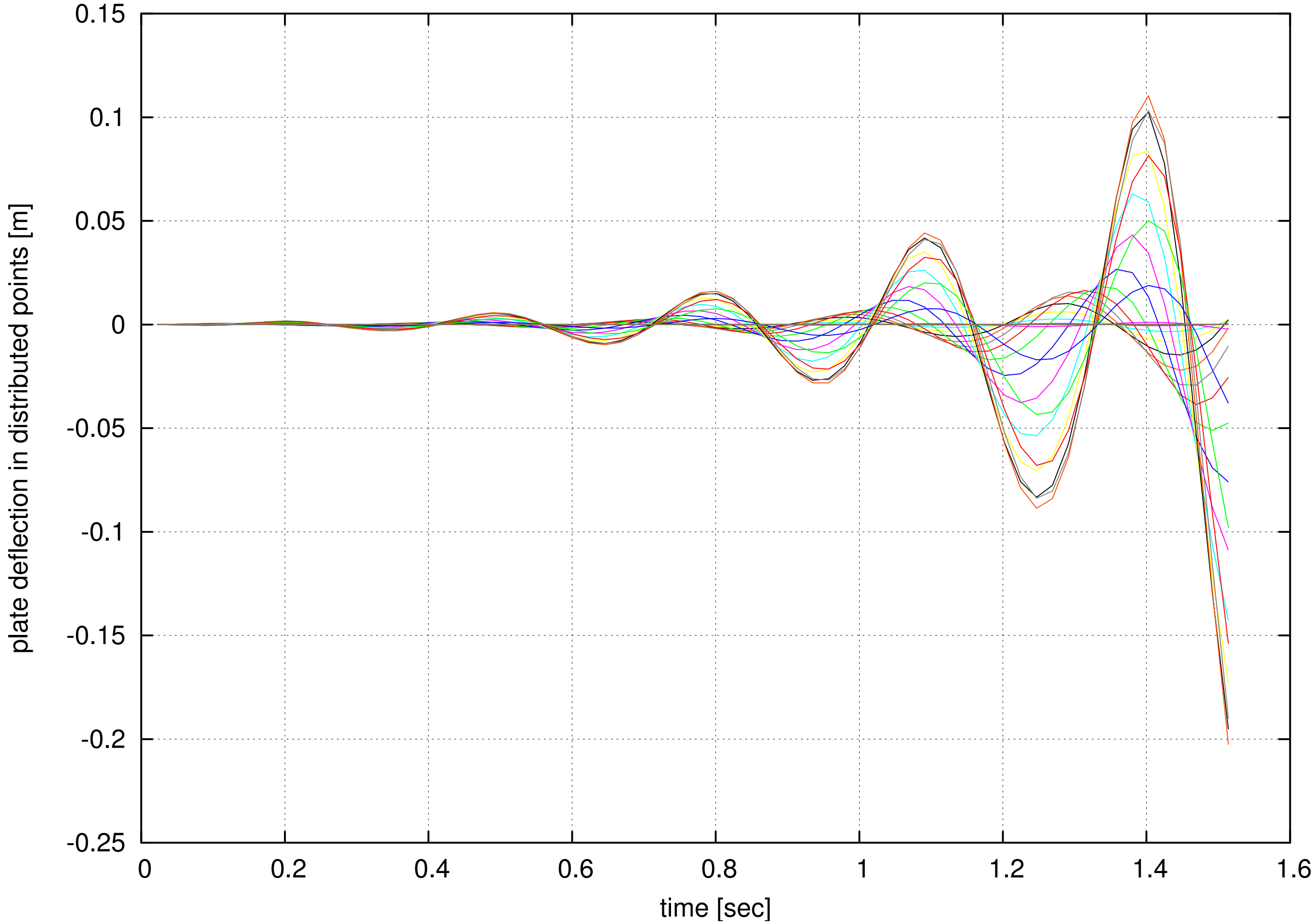

Structure response at M=3.0

Staged FSI-FEM Results for flutter (cont.)

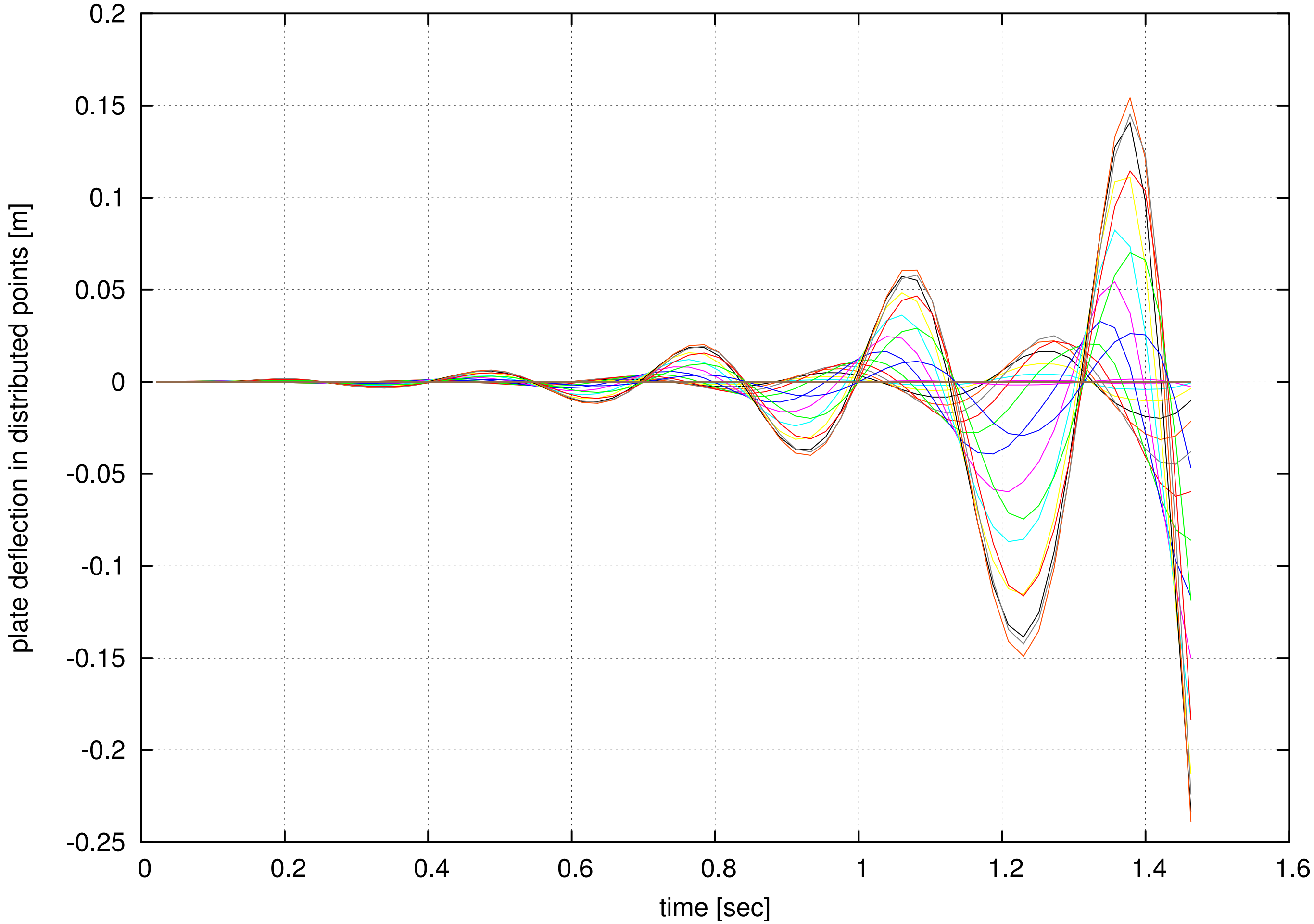

Structure response at M=3.2

Flat plate in flutter

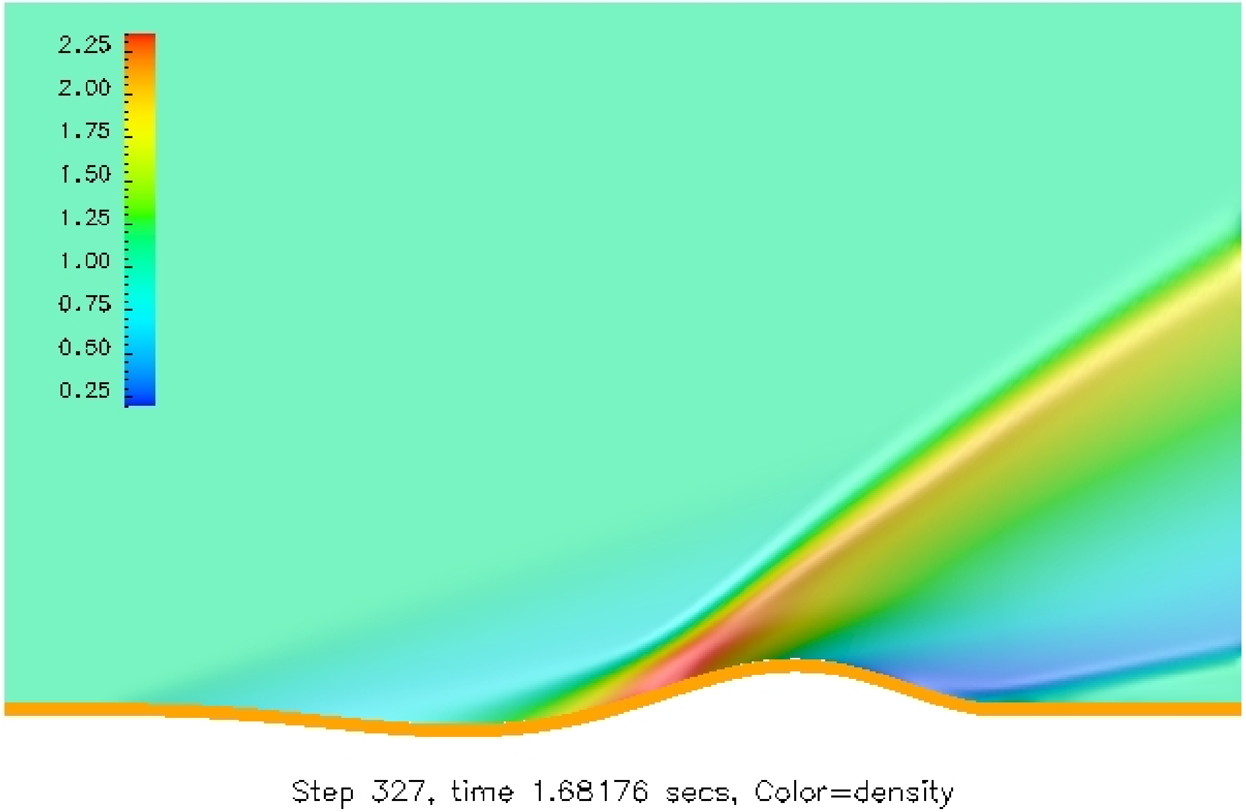

Fluid and Solid fields at $\mathrm{M}_{\infty} = 3.2$

Flat plate in flutter (cont.)

- **Being**

$$\frac{N_M}{N_T \mathrm{M}_\infty{}^2} = \frac{\rho_\infty L^3 c_\infty}{D},$$

sweeps in N_T, N_M and M_∞ estimated the flutter region as

$$\frac{N_M}{N_T \mathrm{M}_\infty{}^2} < 200 \quad \textbf{no flutter for any Mach number},$$

$$\frac{N_M}{N_T \mathrm{M}_\infty{}^2} > 300 \quad \textbf{flutter for the lowest Mach considered } (\mathrm{M}_\infty \geq 1.8).$$

Flat plate in flutter (cont.)

- **If $(\partial u/\partial t)$ is neglected (i.e., characteristic times of struct. are much lower than those of the fluid, $N_T \ll 1$),**

$$\det(\bar{\lambda}^2 \bar{\mathbf{M}} + \mathbf{K} + \mathbf{H}_x) = 0$$

$$\bar{\lambda} = \sqrt{m}\lambda,$$

$$\bar{\mathbf{M}} = \frac{1}{\sqrt{m}} \mathbf{M},$$

the coefficients in $\bar{\mathbf{M}}$, $\mathbf{K}$, $\mathbf{H}_x$ do not depend on m, neither do the eigenvalues of equation, then the λ eigenvalues are of the form

$$\lambda_j = \frac{\bar{\lambda}_j}{\sqrt{m}},$$

with $\bar{\lambda}$ not depending on m. This means that the sign of the real part of the λ is independent of m.

Stability of the staged algorithm

$$U_\infty = \mathrm{M}_\infty = 2$$

$$\mathrm{t} = 0.06,\ \nu = 0.33$$

$$m = 0.002,\ E = 39.6$$

$$D = 8.010^{-4}$$

$$N_T = \frac{D}{mL^2{U_\infty}^2} = 0.025$$

$$N_M = \frac{\rho_\infty L}{m} = 1000.0$$

$$\frac{N_M}{N_T{\mathrm{M}_\infty}^2} = 10000 > 300$$

$$(i.e.,$$

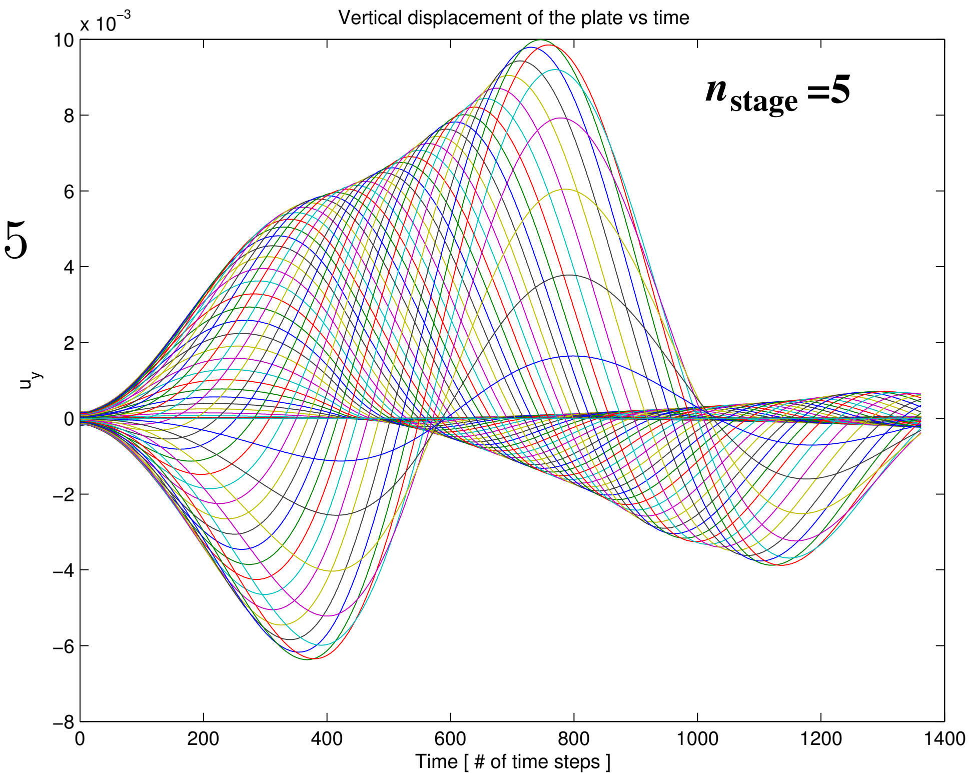

(i.e. inside flutter region)

Stability of the staged algorithm (cont.)

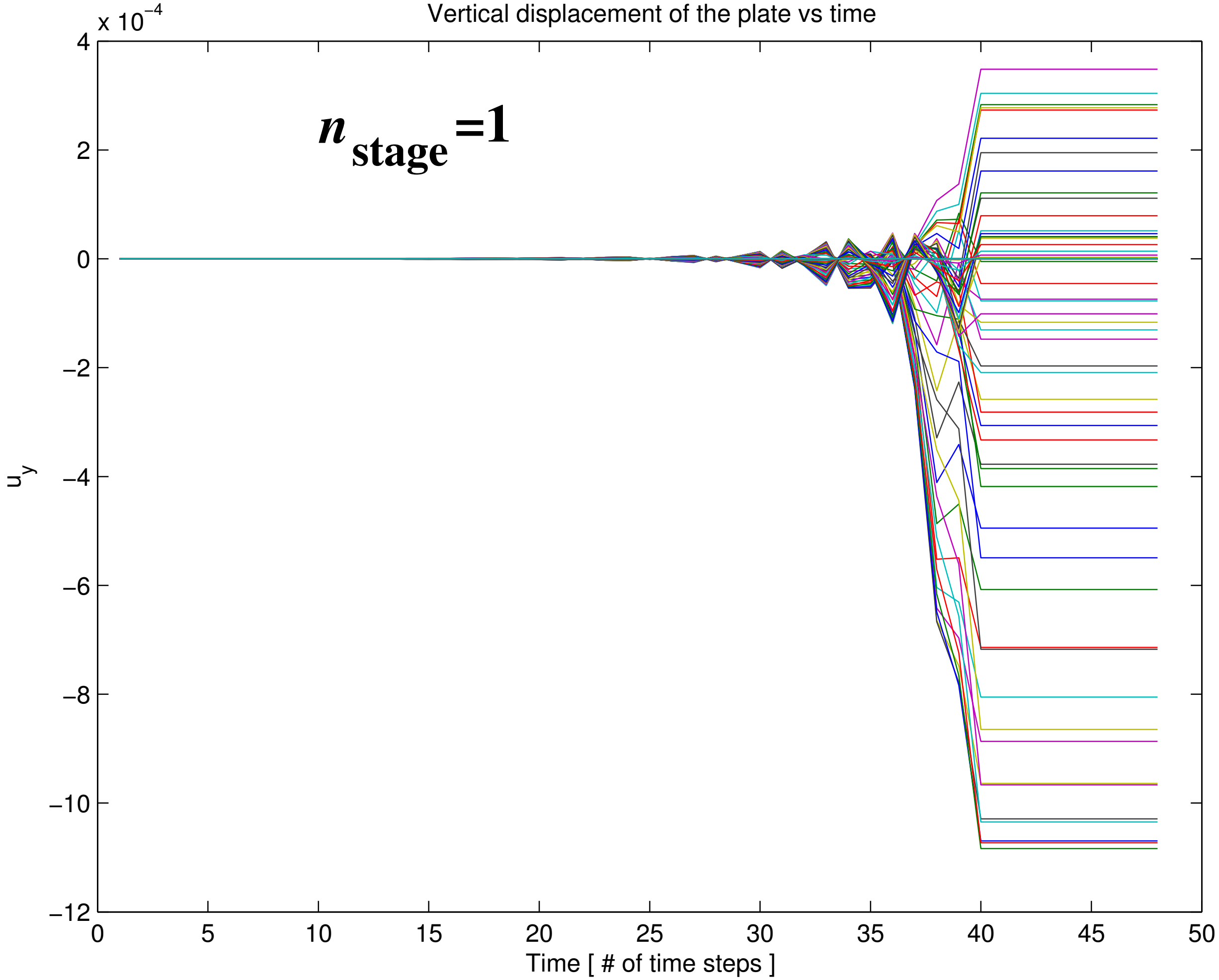

Stability of the staged algorithm (outside flutter region)

- $N_M/(N_T \mathrm{M}_\infty{}^2) \ll 200$
- $N_M/(N_T \mathrm{M}_\infty{}^2)$ **do not depend on plate density** m

$$m = 0.00135$$

$$\frac{N_M}{N_T \mathrm{M}_\infty{}^2} = 12 < 200 \tag{4}$$

(i.e., outsidethe flutter region)

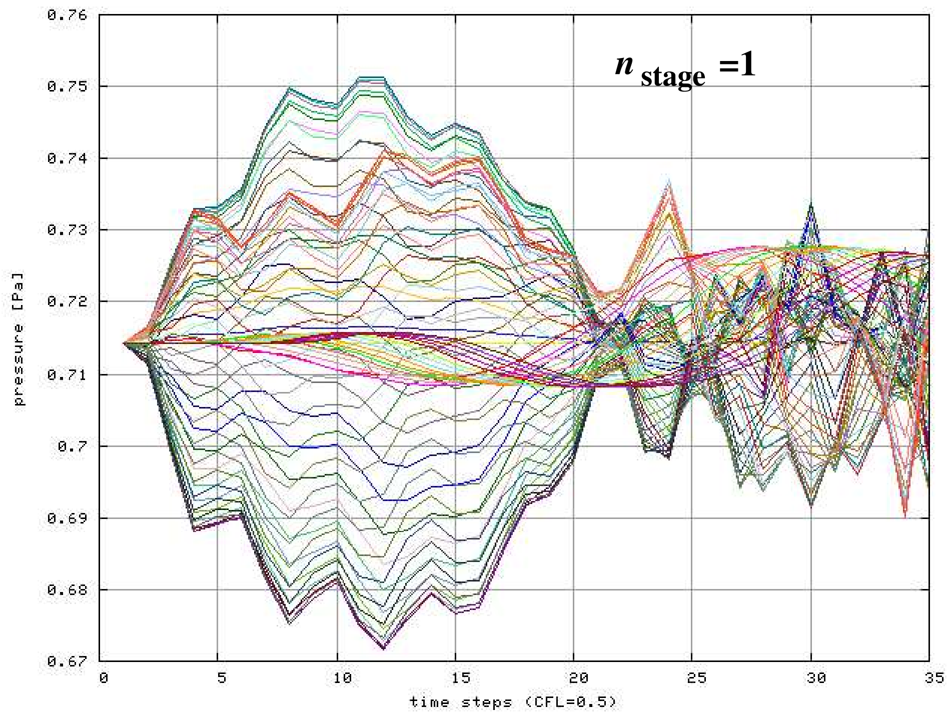

Stability of the staged algorithm (outside flutter region) (cont.)

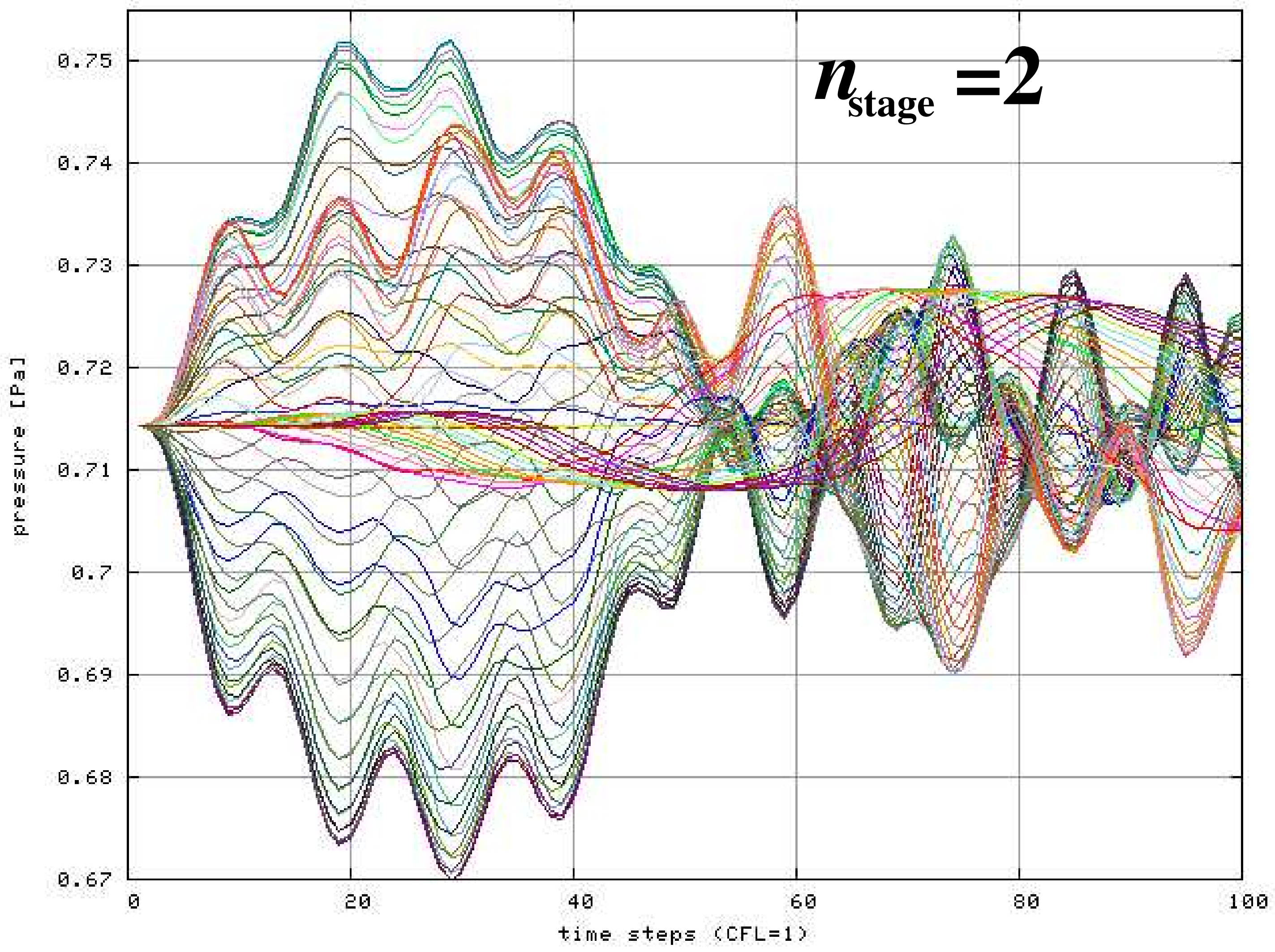

Stability of the staged algorithm (flutter region)

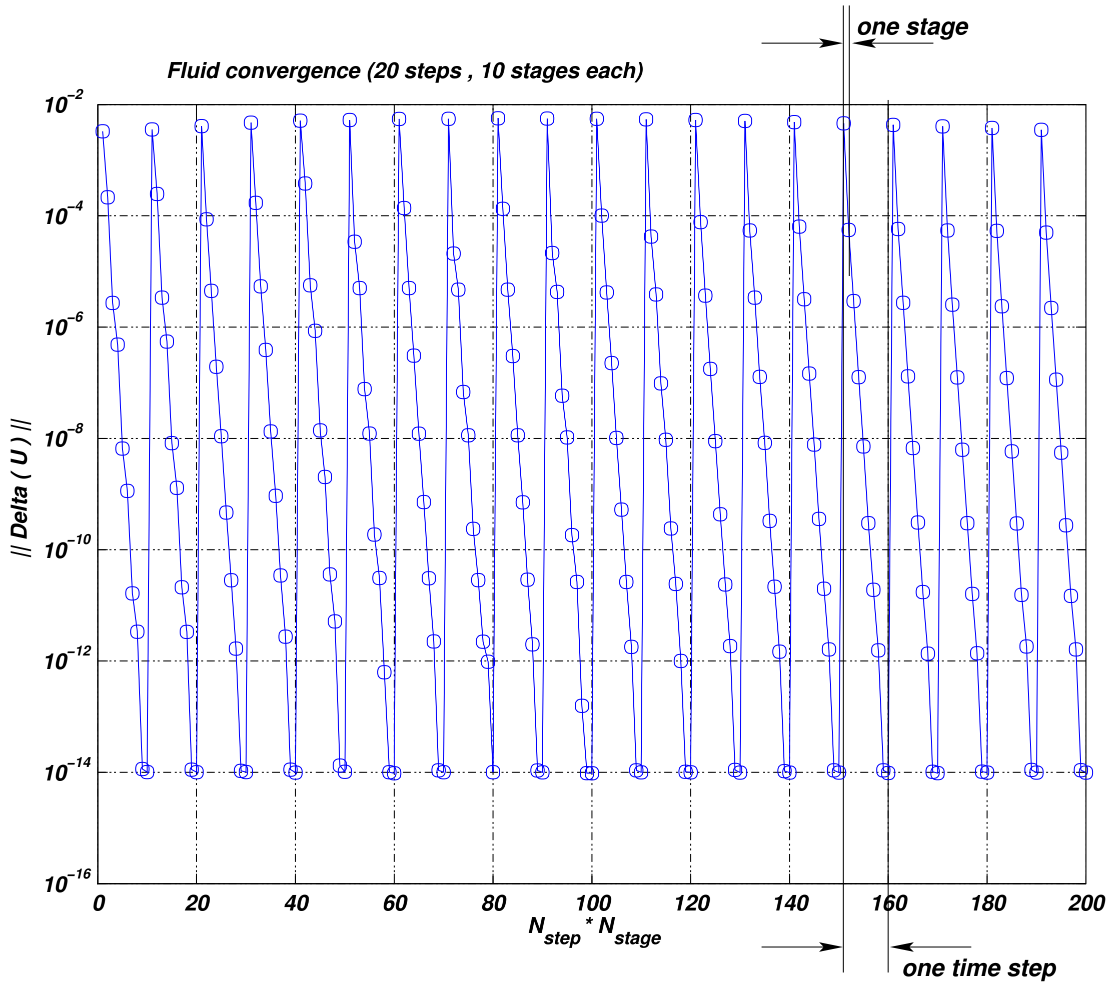

Convergence of fluid state in stage loop

Stability of the staged algorithm (flutter region) (cont.)

- **“Staged” strategy provides a smooth blending between weak coupling and strong coupling.**
- **Moderately coupled problems that can not be treated with the pure weak coupling approach, can be solved with the staged algorithm using few stages per time step.**
- **The elastic flat plate problem is geometrically simple, but gives physical insight in the flutter phenomena, and was very useful in testing the proposed algorithm in a wide range of non-dimensional parameters.**

Aerodynamics of a body falling at supersonic speed

Consider, for simplicity, a two dimensional case of an homogeneous ellipse in free fall. As the body accelerates, the pitching moments tend to increase the angle of attack until it stalls (A), and then the body starts to fall towards its other end and accelerating etc... (*"flutter"*). However, if the body has a large angular moment at (B) then it may happen that it rolls on itself, keeping always the same sense of rotation. This kind of falling mechanism is called *"tumbling"* and is characteristic of less slender and more massive objects.

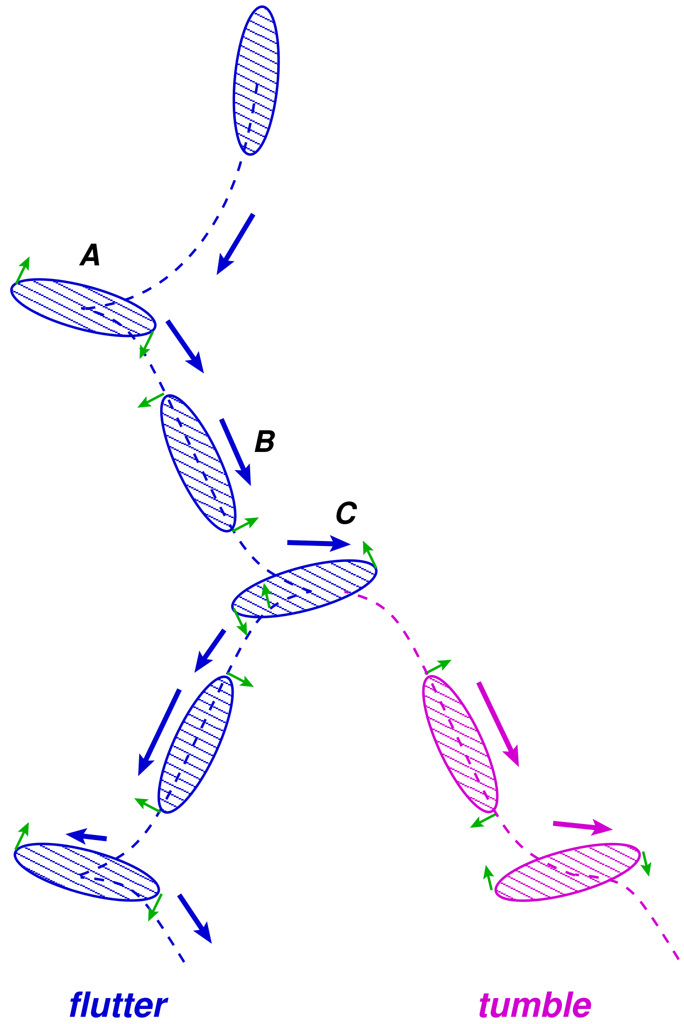

Aerodynamics of a body falling at supersonic speed (cont.)

Under certain conditions in size and density relation to the surrounding atmosphere it reaches supersonic speeds. In particular as form drag grows like L^2 whereas weight grows like L^3, larger bodies tend to reach larger limit speeds and eventually reach supersonic regime. At supersonic speeds the principal source of drag is the shock wave, we use slip boundary condition at the body in order to simplify the problem.

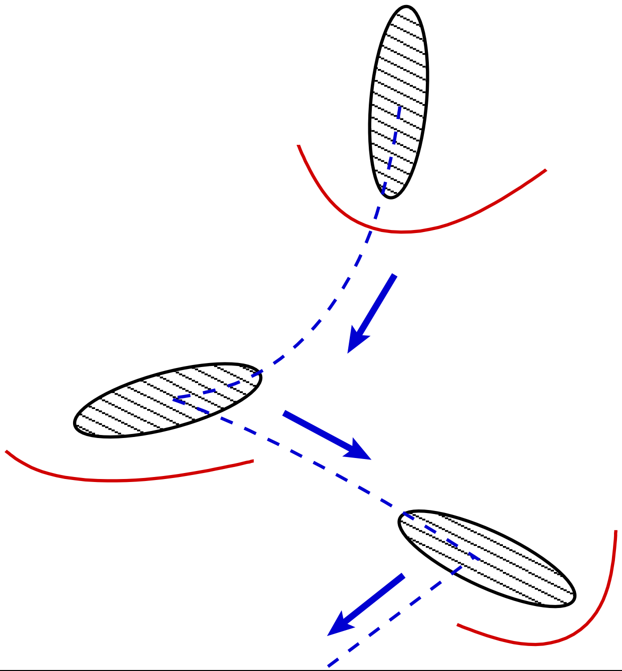

Aerodynamics of a body falling at supersonic speed (cont.)

Params:

- $a = 1$, $b = 0.6$ **(major and minor semi-axes, eccentricity** $e = \sqrt{1 - b^2/a^2} = 0.8$**),**
- $m = 1$, **(mass),**
- $w = 2.5$, **(weight of body),**
- $r = 1$, **(Radius of inertia),**
- $\mathrm{c.m.} = (-0.15, 0.0)$, **(center of mass),**
- $\rho_a = 1$, **(atmosphere density),**
- $p = 1$, **(atmosphere pressure),**
- $\gamma = 1.4$, **(gas adiabatic index** $\gamma = C_p/C_v$**),**
- $R_{\mathrm{ext}} = 10$, **(Radius of the fictitious boundary),**
- $\mathbf{u}_{\mathrm{ini}} = [0, 0, 1.39, 0, 1.3, 0]$, **(ellipse initial position and velocity** $[x, y, \alpha, u, v, \dot{\alpha}]$**),**

Further examples

- **Vortex Induced Vibration (VIV).**
- **Flow impinging a flexible plate.**
- **Incompressible flow in a flexible duct.**
- **Elastically coupled ramp at Mach 6.**

Vortex Induced Vibration (VIV)

- Vortex-induced vibrations (VIVs) of a cylinder at low Reynolds number are presented.
- Main goal is capturing of *synchronization/lock-in* phenomenon when Reynolds number is swept for low dimensionless mass ratio.

- ***mass ratio*** $m^* = 153.3524$
- ***frequency ratio*** $F_n = 0.1766$
- ***damping ratio*** $\zeta = 0.5857$
- ***Reynolds number*** $Re \in (90, 150)$

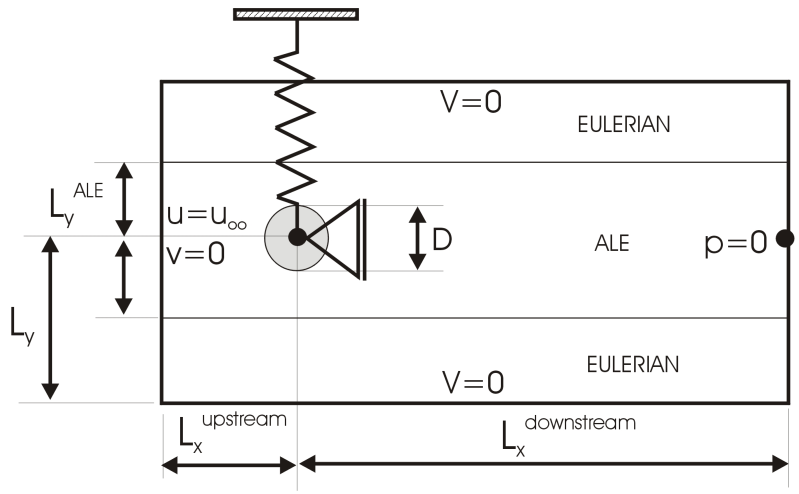

Vortex Induced Vibration (VIV) (cont.)

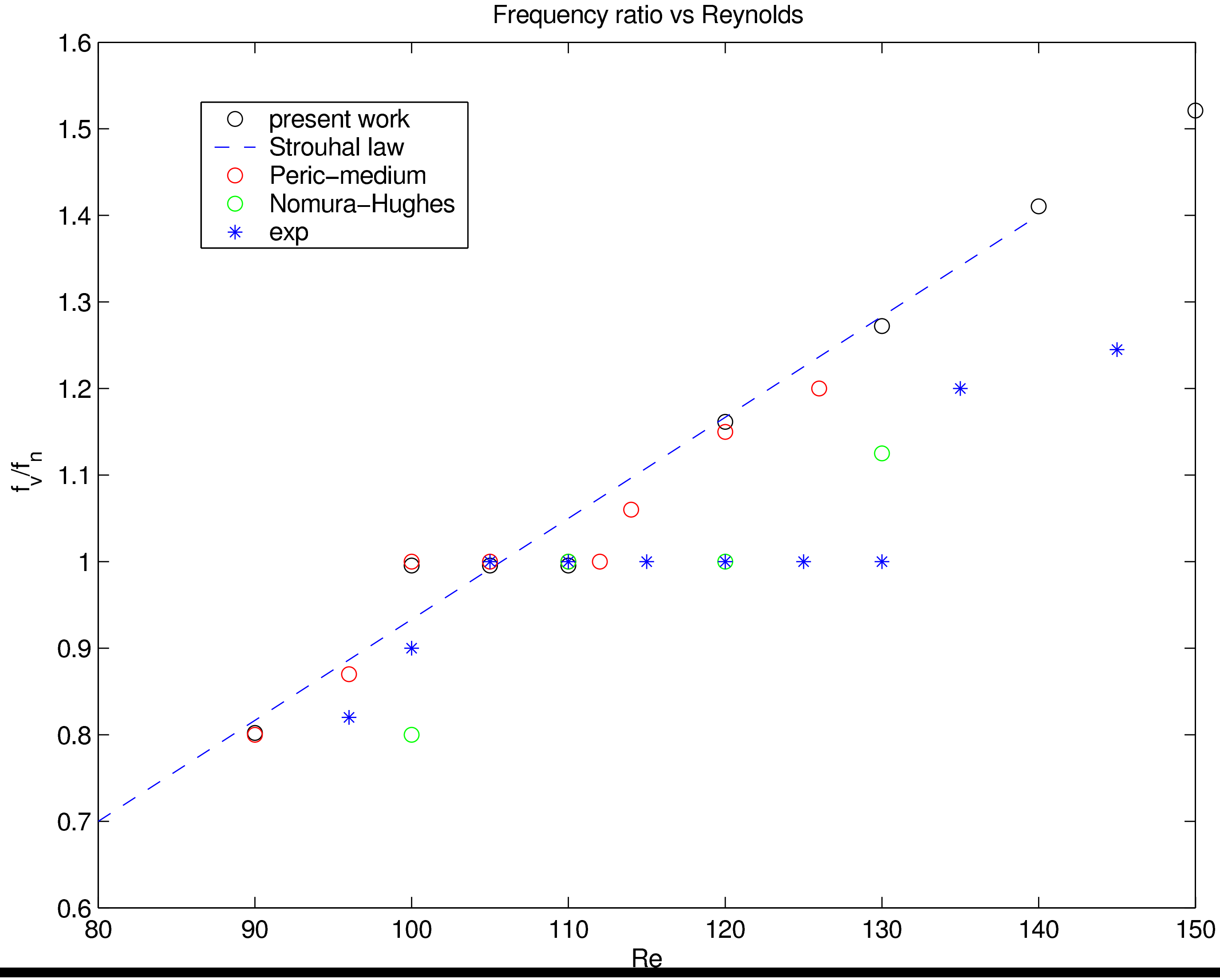

Vortex Induced Vibration (VIV) (cont.)

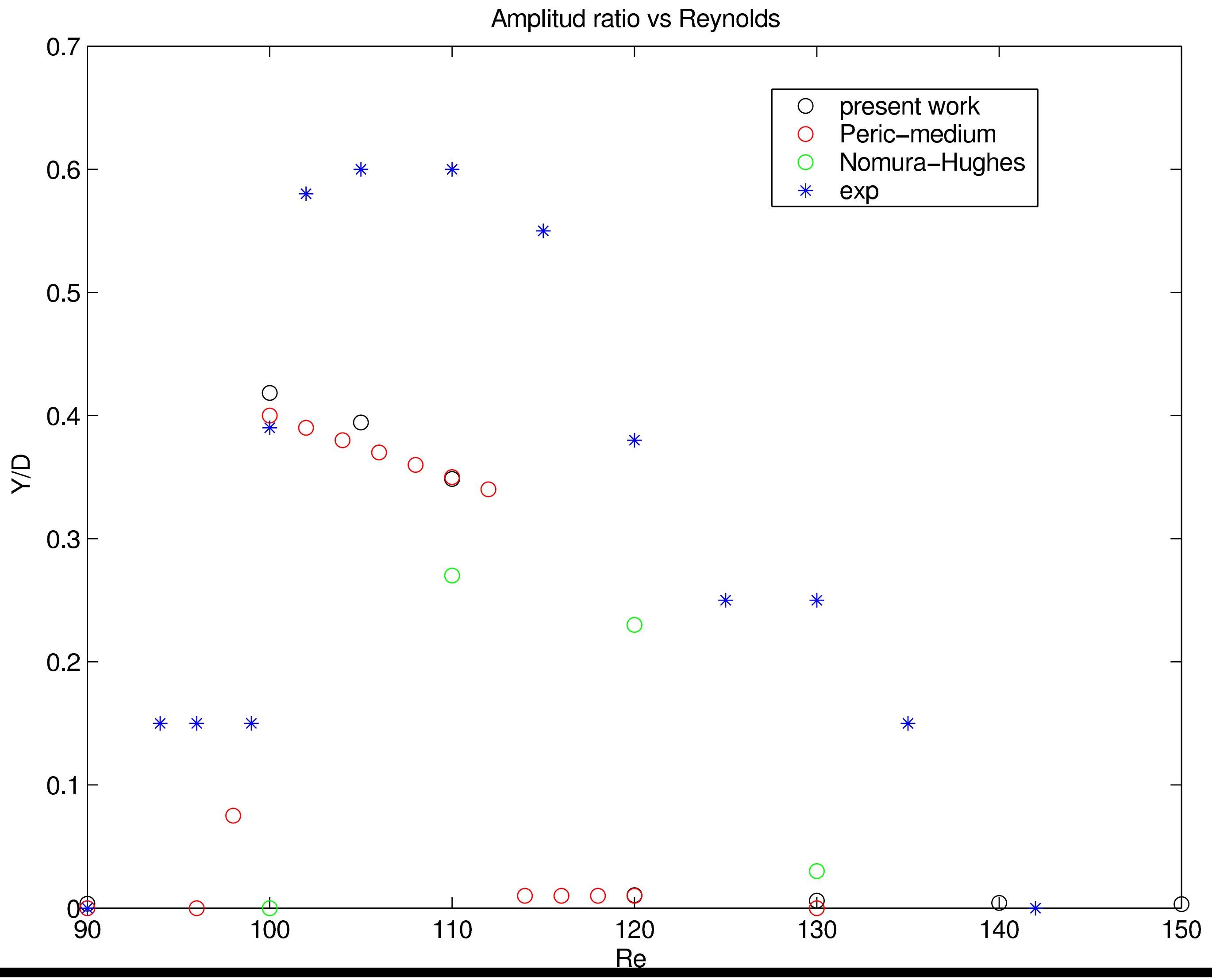

Vortex Induced Vibration (VIV) (cont.)

- **monolithic (blue star) - 2nd order**
- **staggered with no predictor (black circle) - 1st order**
- **staggered with predictor** $\alpha_0 = 1$ $\alpha_1 = 0$ **(cyan star) - 1st order**

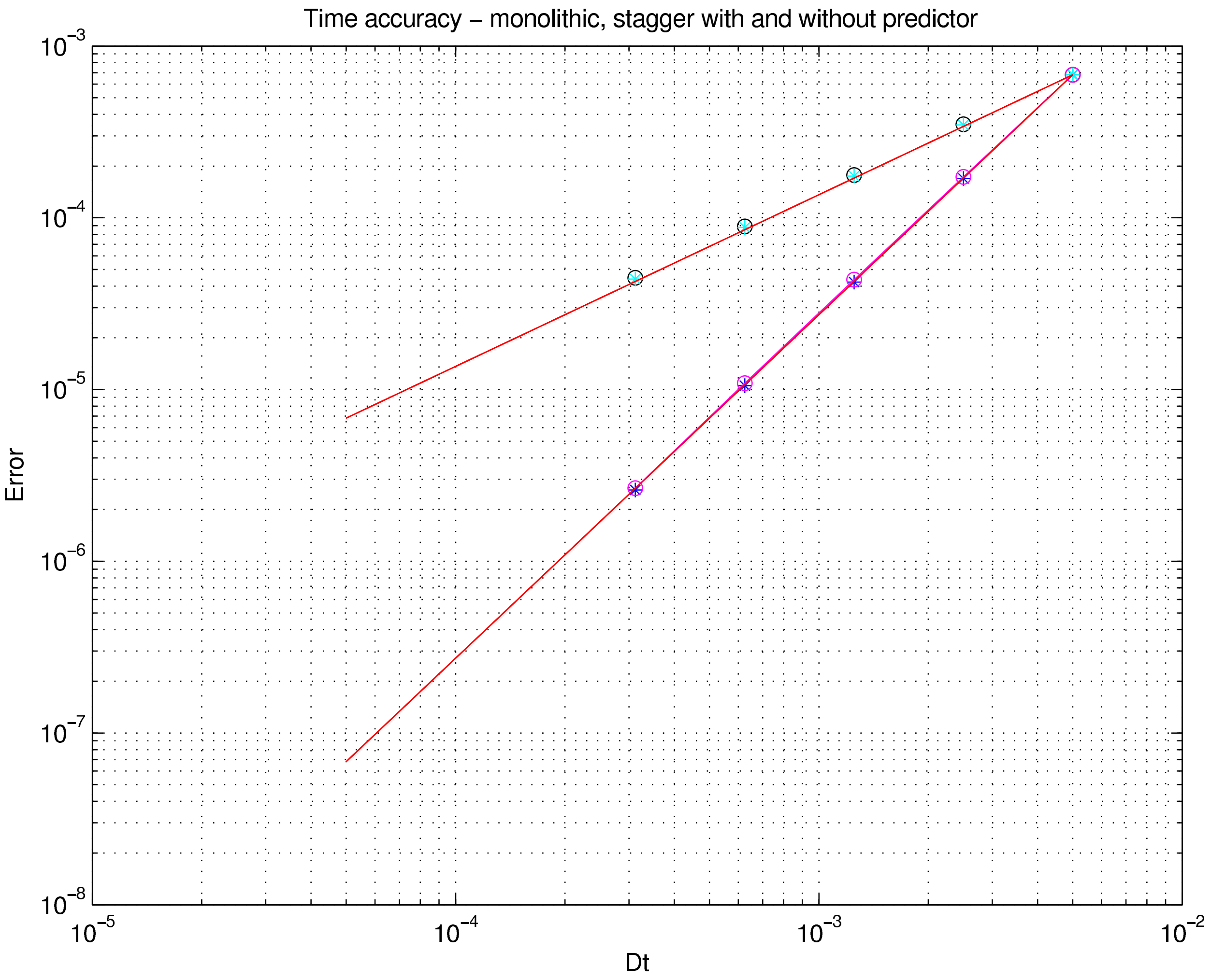

Flow impinging a flexible plate

Proposed in Tam & Radovitzky ("An algorithm for modelling the interaction of a flexible rod with a two-dimensional high-speed flow", Int J Num Meth Engng, 2005, pp. 1057-1077). The simulation corresponds to a supersonic flow transverse to an initially-flat structure made of an elastic fabric.

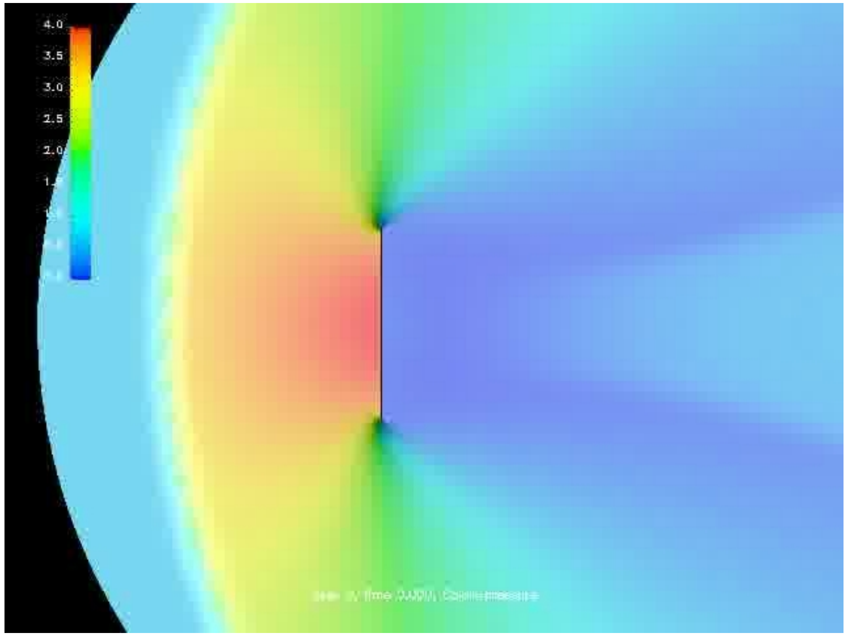

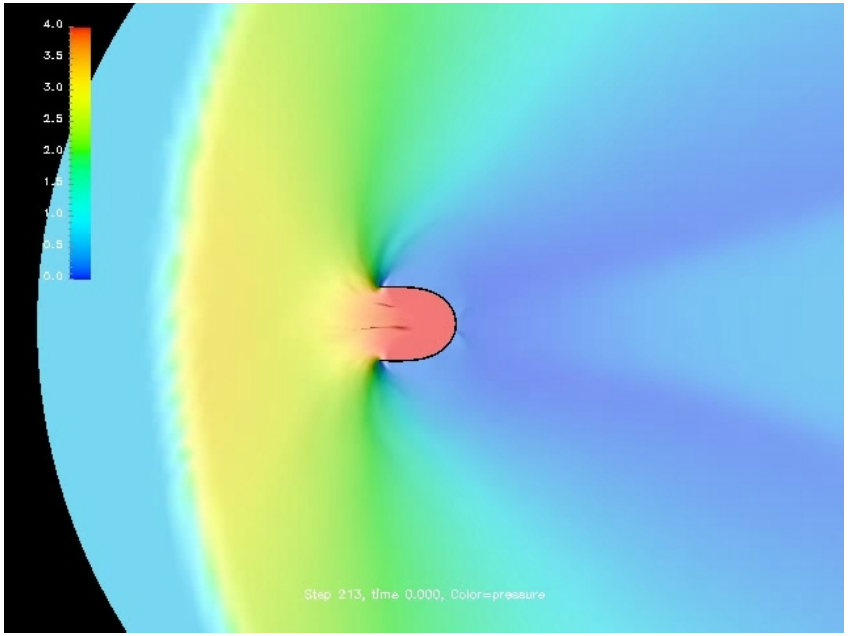

Flow impinging a flexible plate (cont.)

- **solid Young's Modulus** $E = 6\times 10^9 \mathrm{Pa}$**,**
- **solid density** $\rho_{\mathrm{sol}} = 1000.0kg/\mathrm{m}3$**.**
- **The length of the structure is** $L = 1\mathrm{m}$**,**
- **Moment of inertia** $I = h^3/(12(1-\nu^2)) = 2.25\times 10^{-9}\mathrm{m}^3$**, where** $h = 0.003\mathrm{m}$ **is the thickness of the plate.**
- **For the fluid upstream pressure** $p = 1.0\mathrm{atm}$**,**
- **fluid mass density** $\rho = 1.293\mathrm{kg}/\mathrm{m}^3$**,**
- **fluid adiabatic index** $\gamma = 1.4$**.**
- **The fluid income Mach number is** $\mathrm{M} = 2.0$**.**

Flow impinging a flexible plate (cont.)

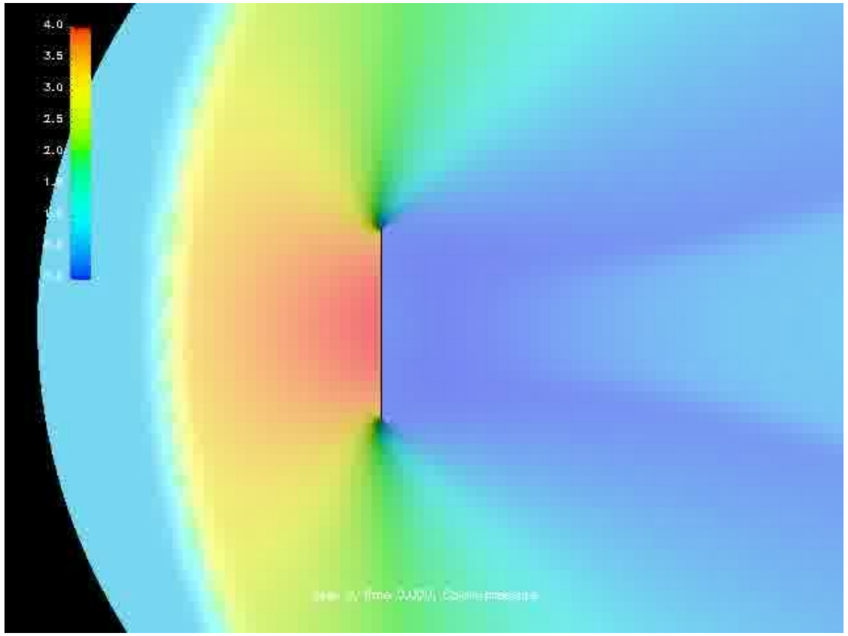

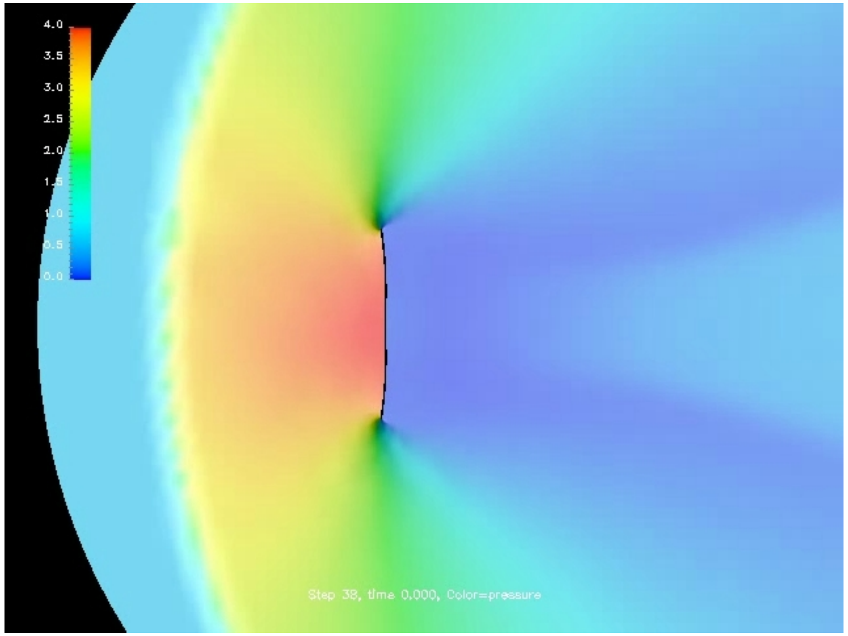

Flow impinging a flexible plate (cont.)

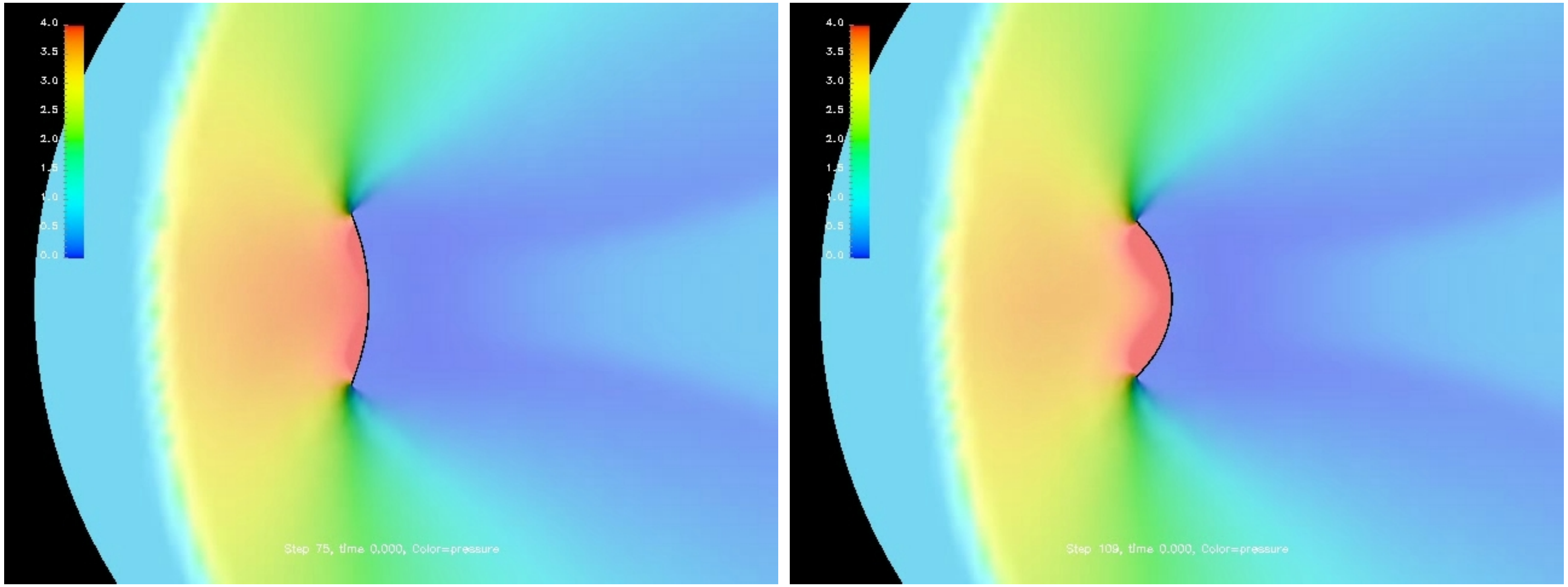

Flow impinging a flexible plate (cont.)

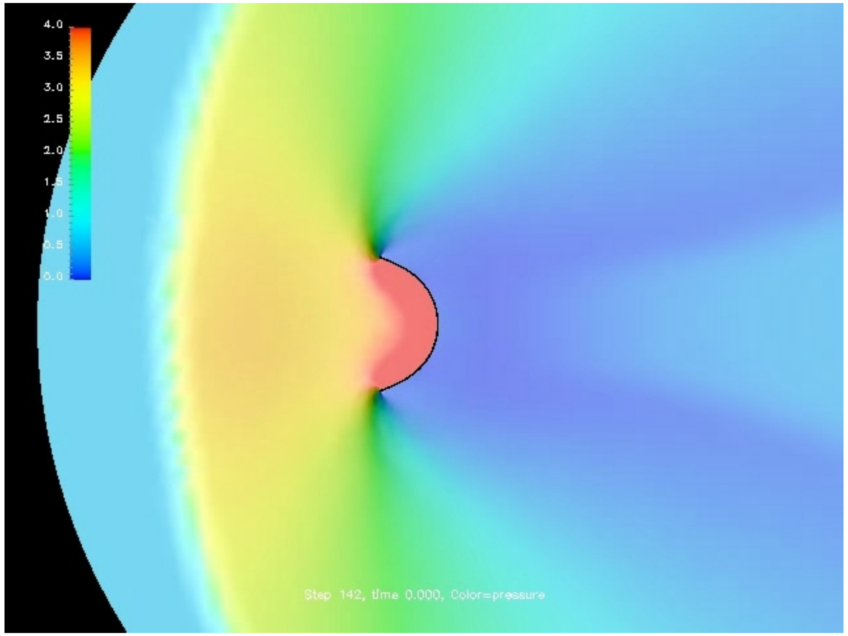

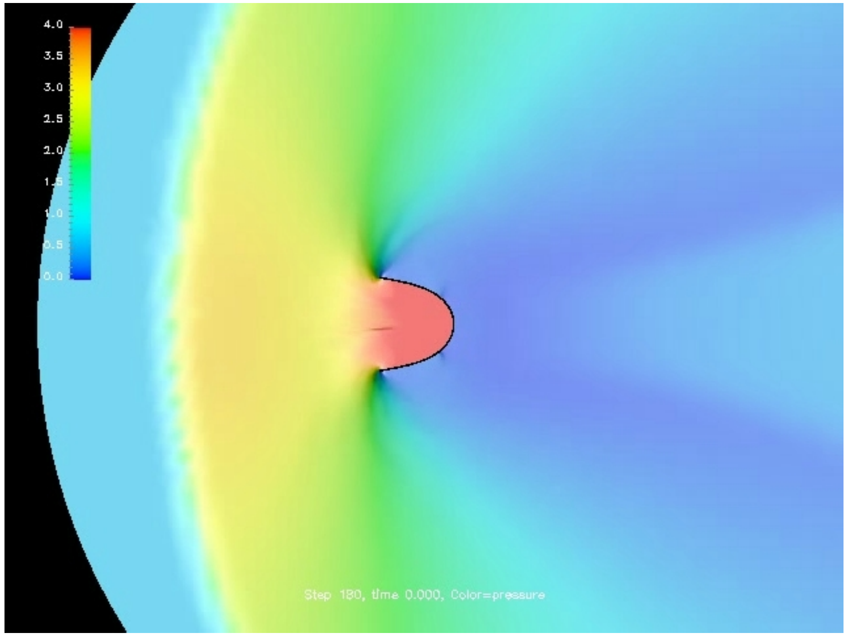

Flow impinging a flexible plate (cont.)

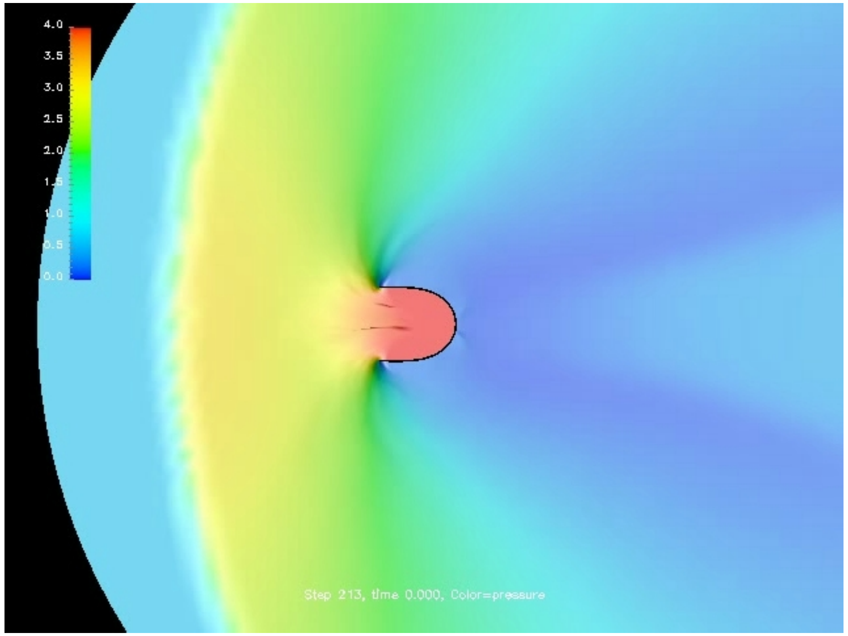

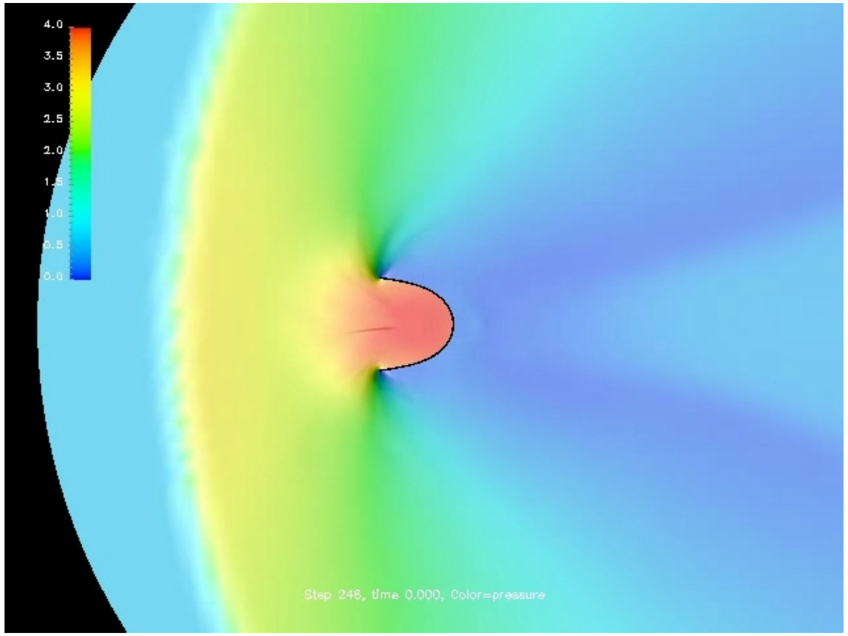

Flow impinging a flexible plate (cont.)

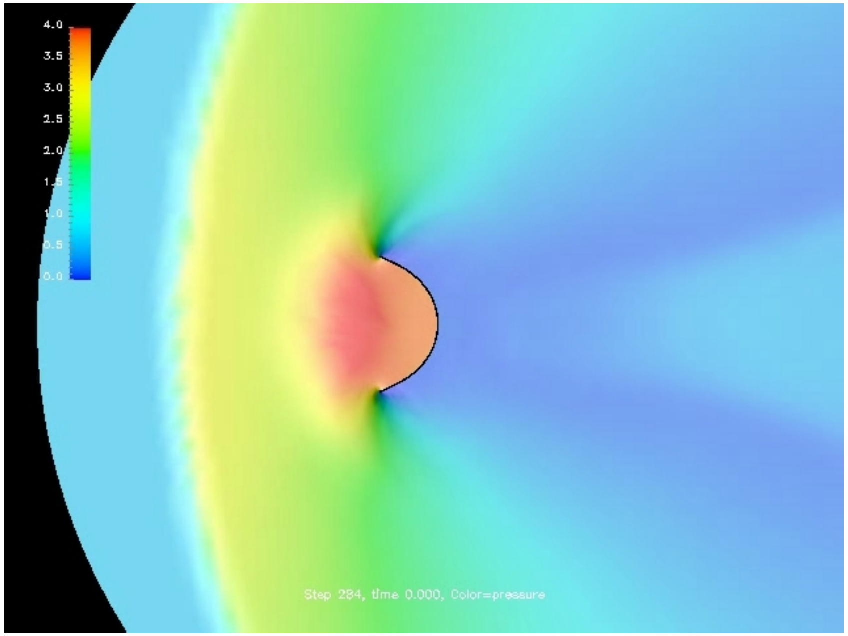

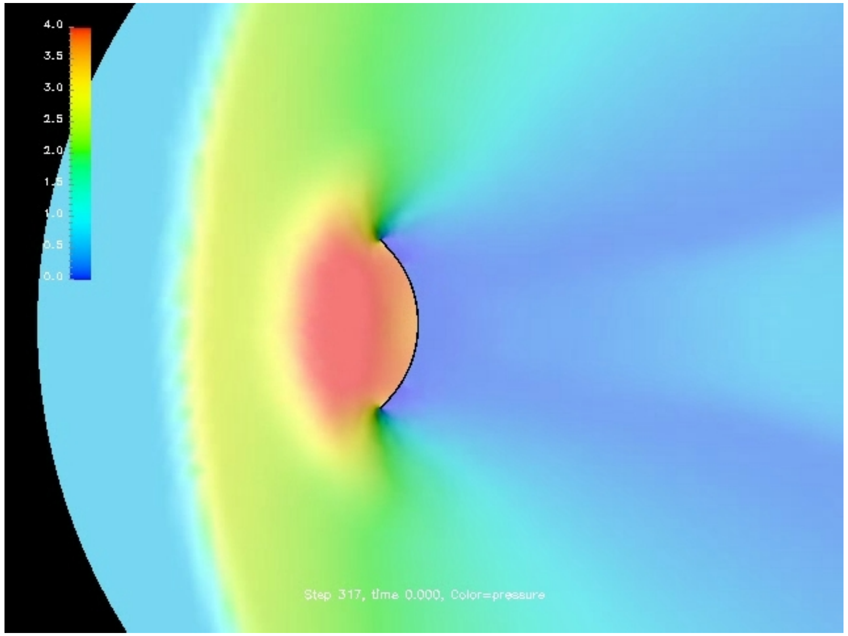

Flow impinging a flexible plate (cont.)

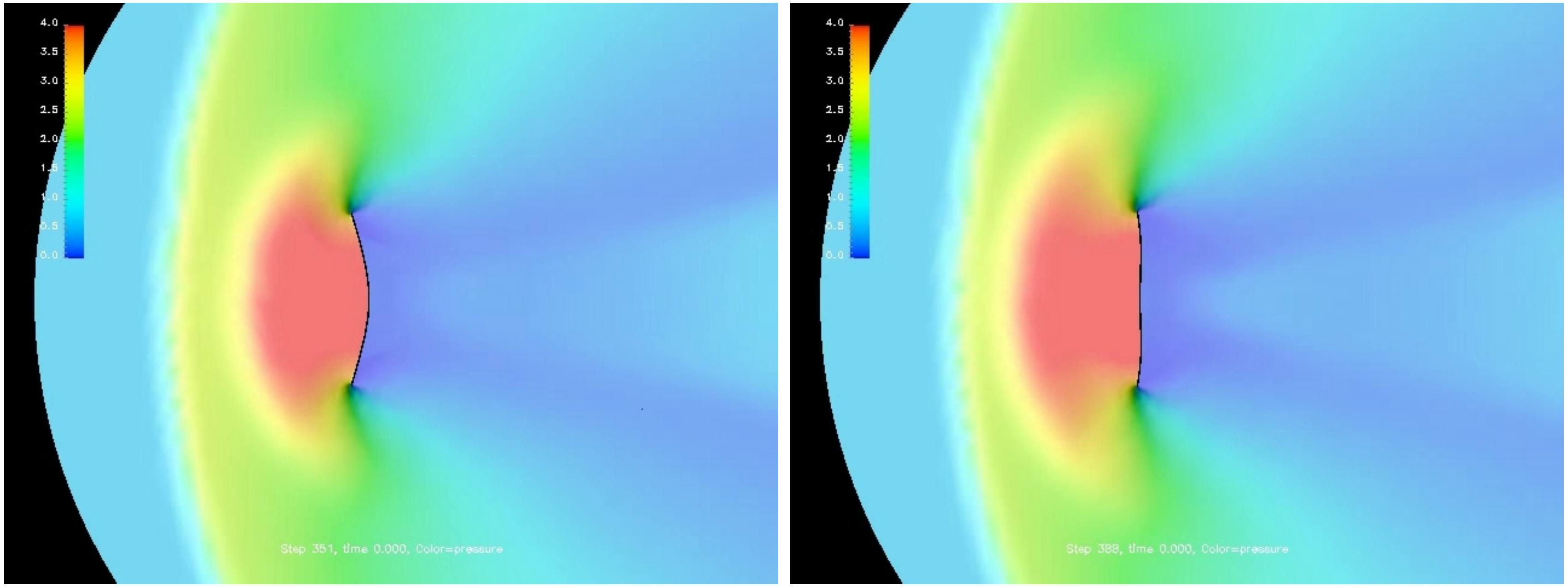

Flow impinging a flexible plate (cont.)

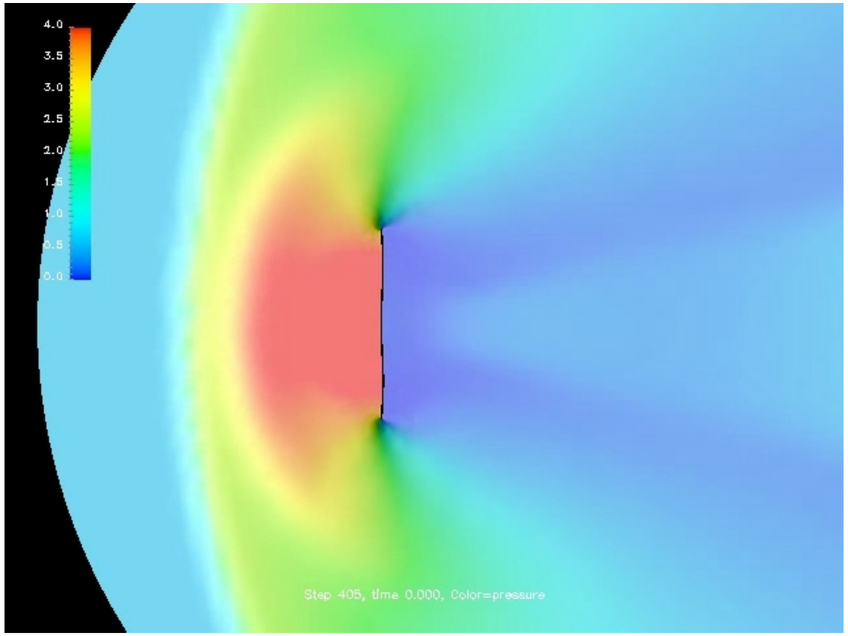

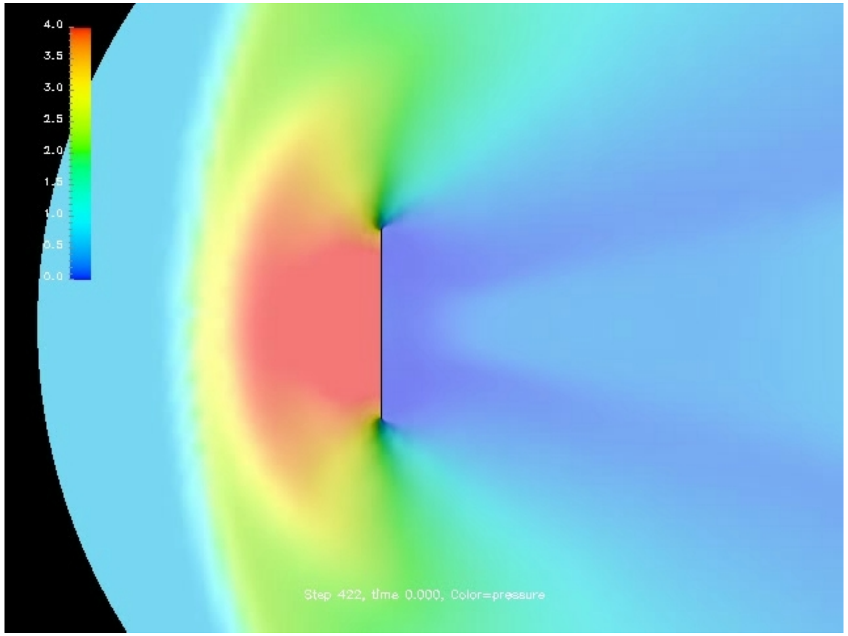

Flow impinging a flexible plate (cont.)

The flow ins inviscid and slip conditions are assumed on the skin of the plate. Initially, the steady flow is established for the plate at a rigid position and a bow shock of intnesity $p_{\rm stag}/p_\infty > 5$ is formed. Then the plate is released to bend freely, with the constraint that the plate ends can only slide in the vertical direction. Due to the high difference of pressure between both sides of the plate, it initially bends. An expansion fan is formed behind the plate, during this initial phase. After a point of maximum bending is reached the stiffness of the plate starts to react and the plate straightens to its original position. During this phase the plate reaches supersonic velocities and a second shock is formed behind the plate. Some frames are shown in the following figures.

Incompressible flow in a flexible duct

The computational domain is, initially, a circular cylinder $r = \sqrt{y^2 + z^2} \leq R_{\rm in}$, $0 \leq x \leq L_{\rm duct}$ for the fluid and a cylindrical duct $R_{\rm in} \leq r \leq R_{\rm ext}$, $0 \leq x \leq L_{\rm duct}$ for the structure. A large deformation compressible elastic model has been adopted for the structure.

The boundary conditions are, for the fluid

- **non-slip at the fluid-structre interface boundary,**
- $w_x = (\bar{w}_x + \Delta w_x \, \cos(\omega t))(1 - r^2/{R_{\rm in}}^2)$, $w_y = w_z = 0$**, at the inlet (**$x = 0$**), i.e. parabolic profile with sinusoidally varying amplitude, with mean** $\bar{w}_x$ **and fluctuation** Δw_x**,**
- $p = p_{\rm ref}$ **at outlet (**$x = L_{\rm duct}$**),**

Incompressible flow in a flexible duct (cont.)

For the structure,

- $u_x = 0$ **at both ends (**$x = 0, L_{\rm duct}$**), i.e. the nodes at the ends can slide in the** $y - z$ **plane,**
- **Tractions taken from the fluid at the fluid-structure interface.**
- $\sigma = -p_{\rm ref}\mathbf{I}$ **at the exterior wall.**

The stiffness of the structure varies with x **so that a certain portion in the middle (**$x_1 \leq x \leq x_2$**) is weaker (lower Young modulus) than the rest. The experiment simulates the phenomena associated with aneurisms in blood vessels. The weaker portion of the duct blows periodically with the pulsating incoming flow.**

Incompressible flow in a flexible duct (cont.)

The parameters are

- $L_{\rm duct} = 5$,
- $R_{\rm in} = 1$,
- $R_{\rm ext} = 1.1$, **(wall thickness $t = 0.1$),**
- $E = 1000$, **(Young modulus),**
- $E_{\rm weak} = 300$, **(Young modulus at weaker part of duct),**
- $x_1 = 1, x_2 = 3.25$, **(weak portion of duct),**
- $\rho_{\rm solid} = 2$, **(solid density),**
- $\nu = 10^{-4}$, **(fluid viscosity),**
- $\bar{w}_x = 1$, **(mean velocity at axis),**
- $\Delta w_x = 0.3$, **(velocity perturbation at axis),**
- $\Delta t = 0.02$, **(time step),**
- $\omega = 2\pi/T_{\rm pulse}$, $T_{\rm pulse} = 8$, **(pulse period),**

Incompressible flow in a flexible duct (cont.)

The following results have been obtained with a mesh of composed of 19602 hexahedral elements in a circumferential slice of 15°. Periodic boundary conditions have been imposed on the opposite sides of the slice. Some results (animations/colormaps) are shown in 3D extruding the axisymmetrical results.

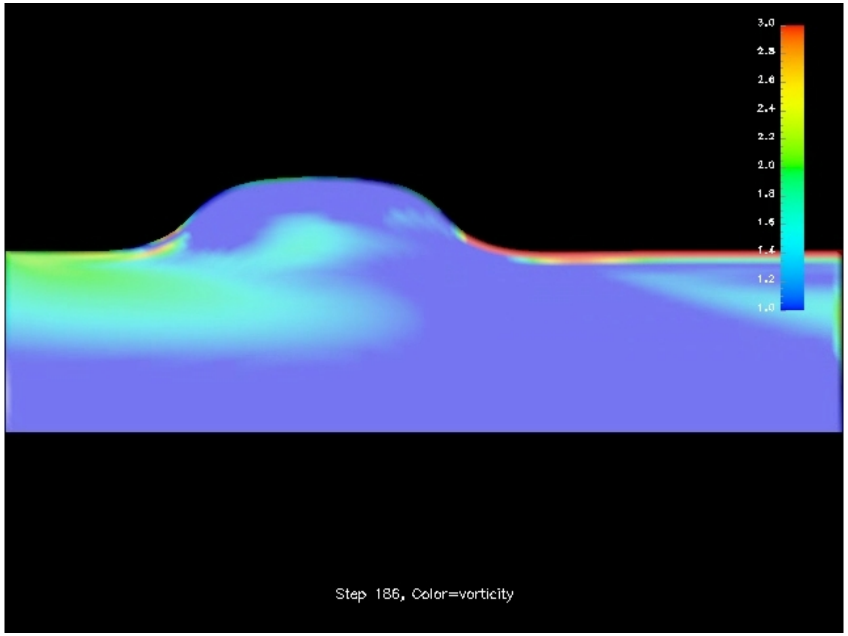

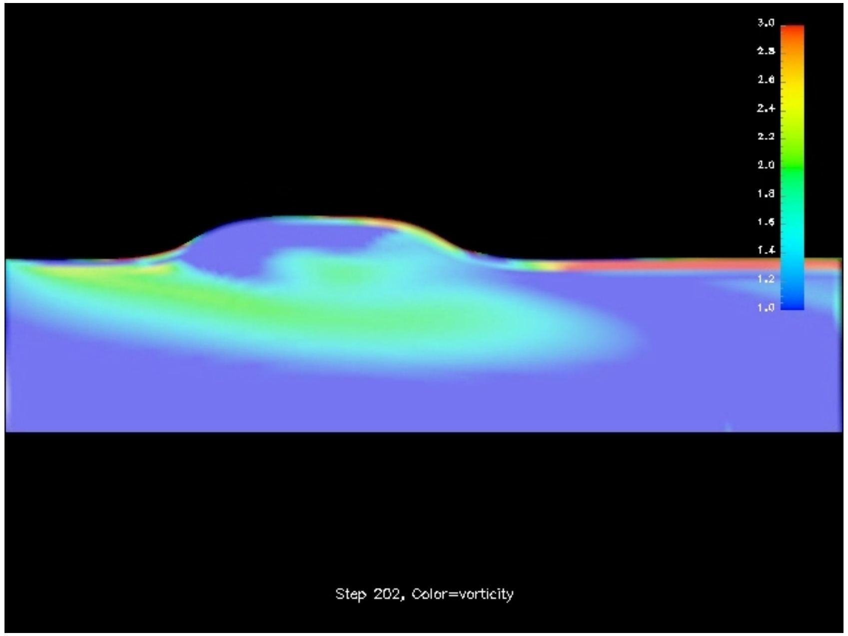

Incompressible flow in a flexible duct (cont.)

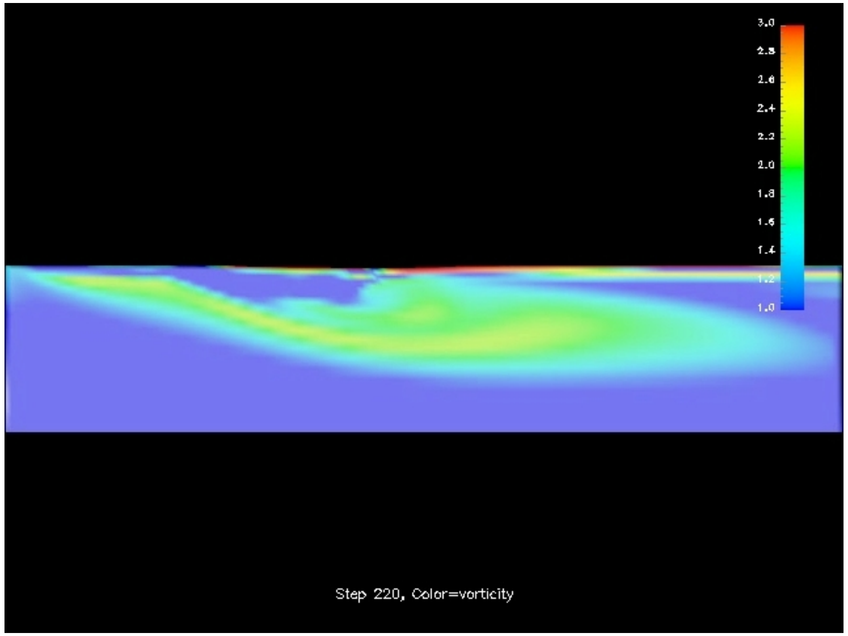

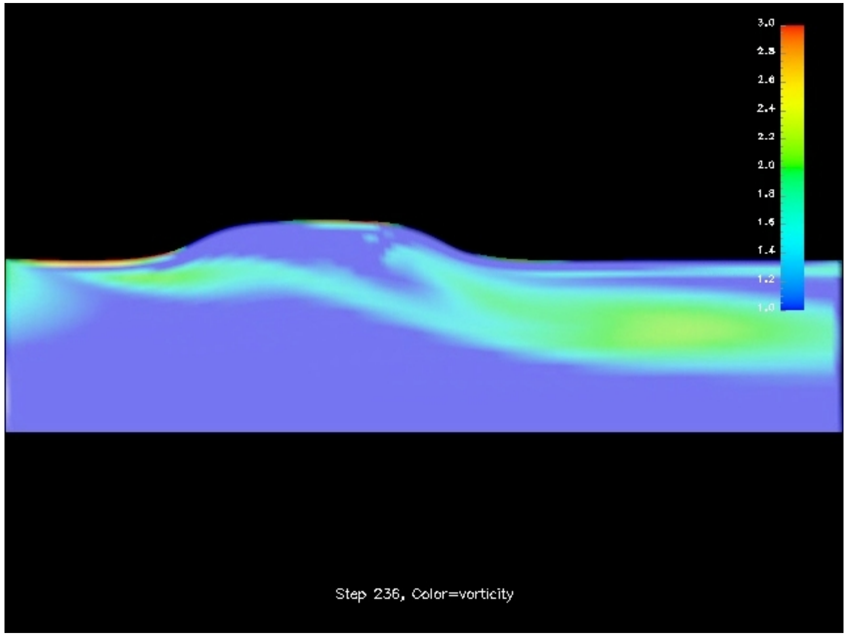

Incompressible flow in a flexible duct (cont.)

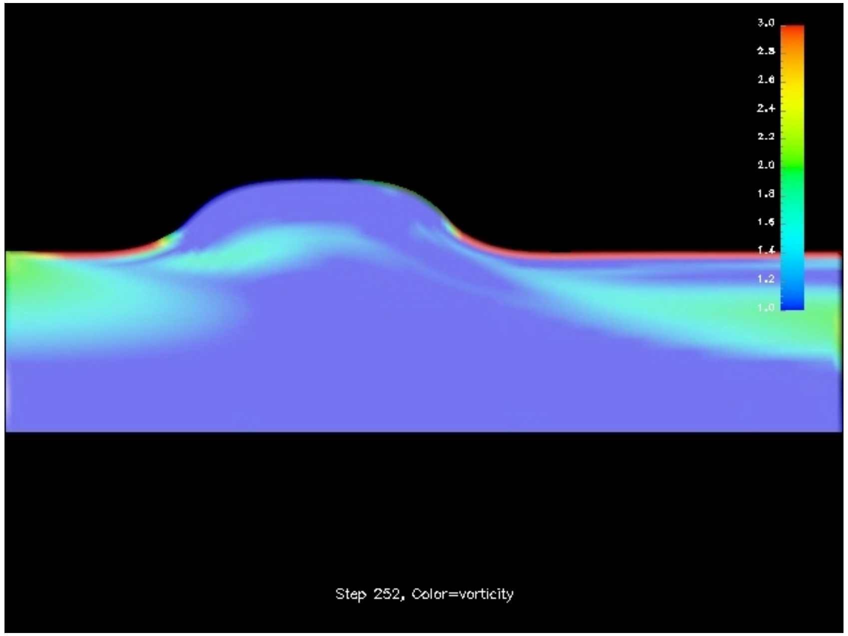

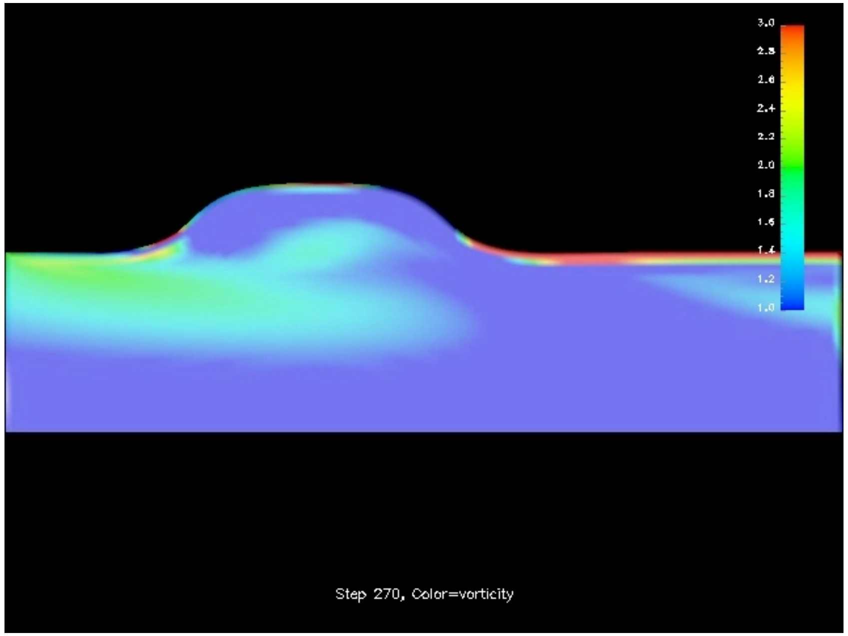

Incompressible flow in a flexible duct (cont.)

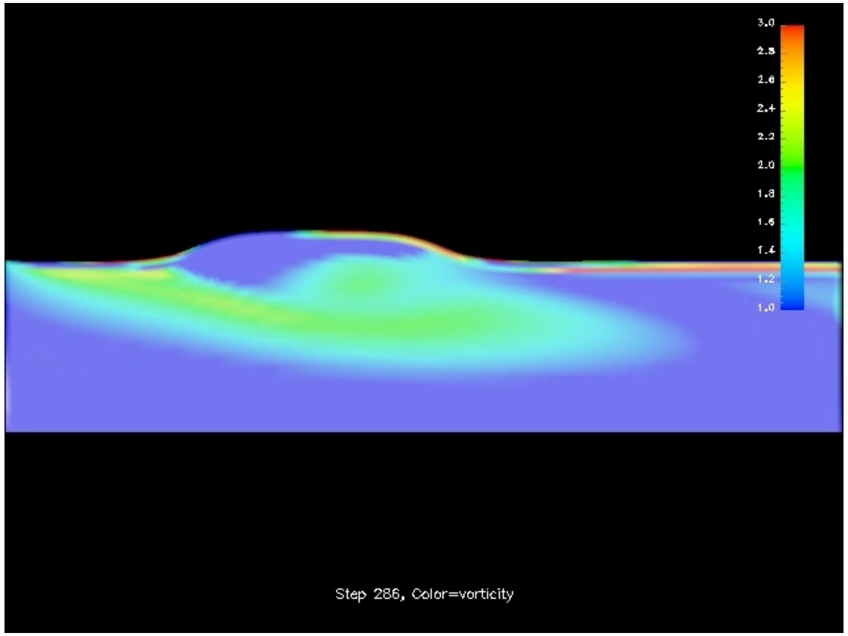

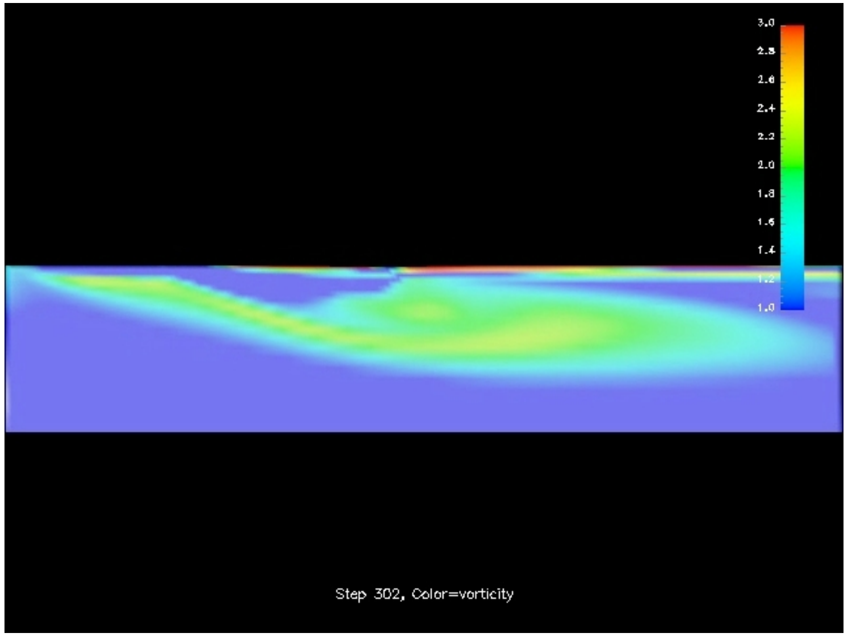

Elastically coupled ramp at Mach 6

The test is based on the inviscid ramp test benchmark, but now the ramp is elastically articulated at the corner.

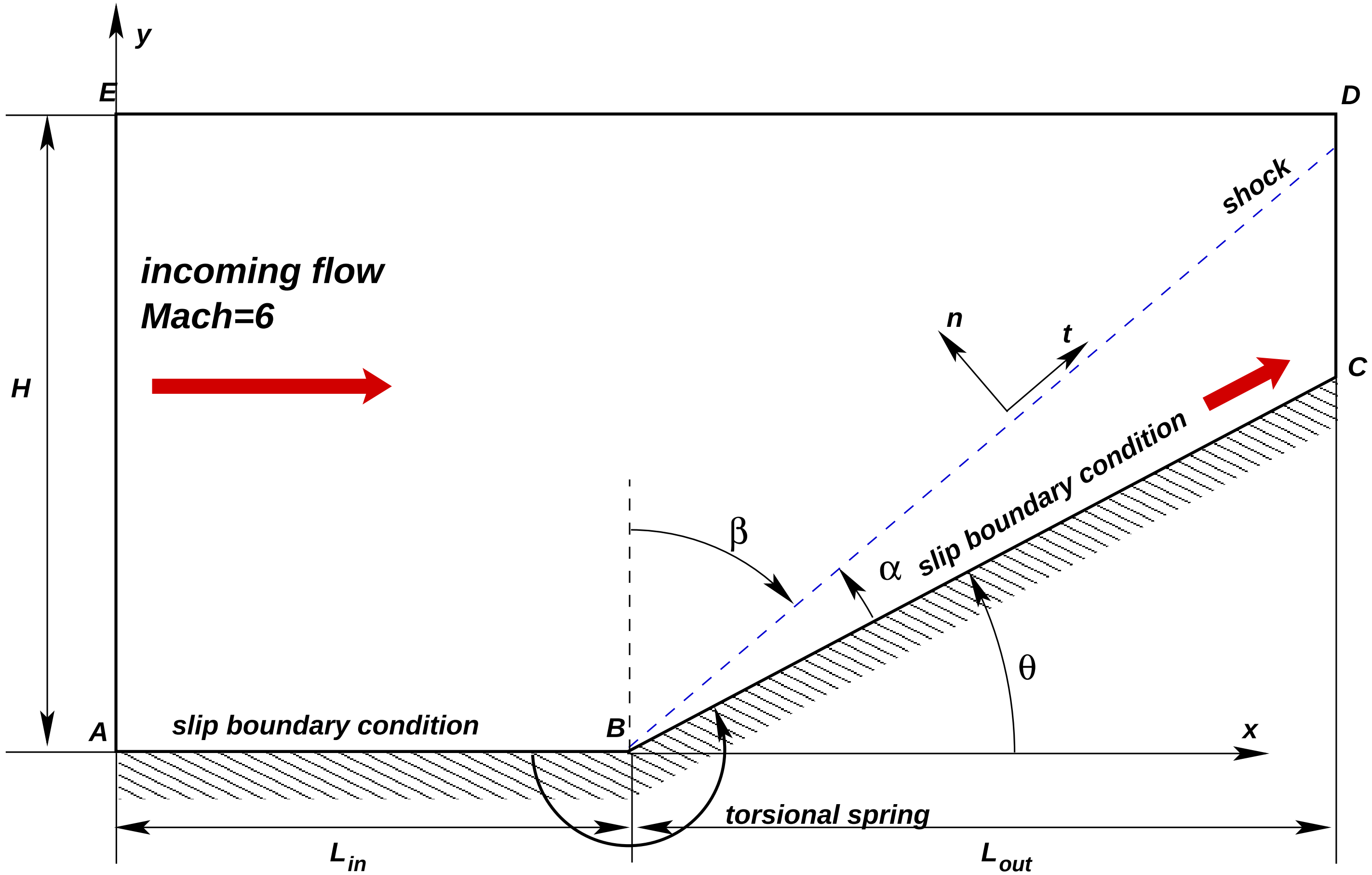

Elastically coupled ramp at Mach 6 (cont.)

Ths spring constant is $K = 10^7 \mathrm{Nm}$. The value of deflection in the steady state is $\theta_0 - \theta = 1.52^\circ$. The analytical value is $\theta_0 - \theta = 1.54^\circ$. The pressure behind the shock is 3.75660 (dimesional: 525924 [Pa]), i.e. a pressure ratio of 5.259 which is within 0.3% of the analytical value presented previously.

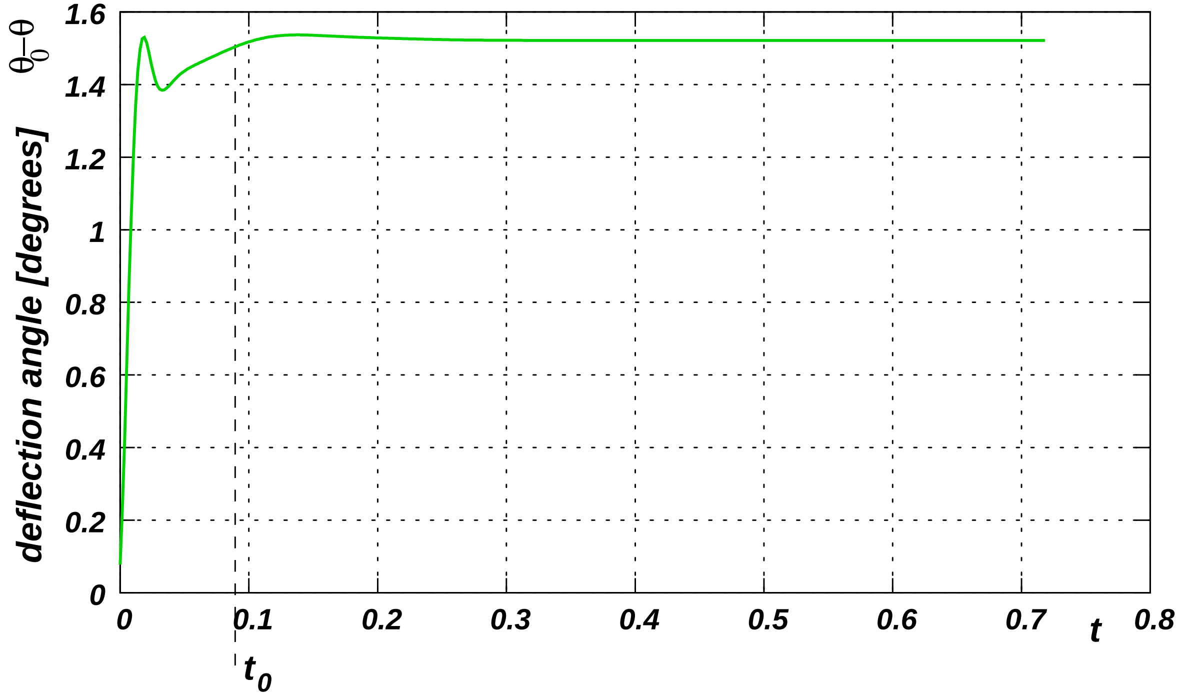

Elastically coupled ramp at Mach 6 (cont.)

In order to get a larger deflections we modified the torsional spring constant to $K = 2\times 10^6\,\mathrm{Nm}$.

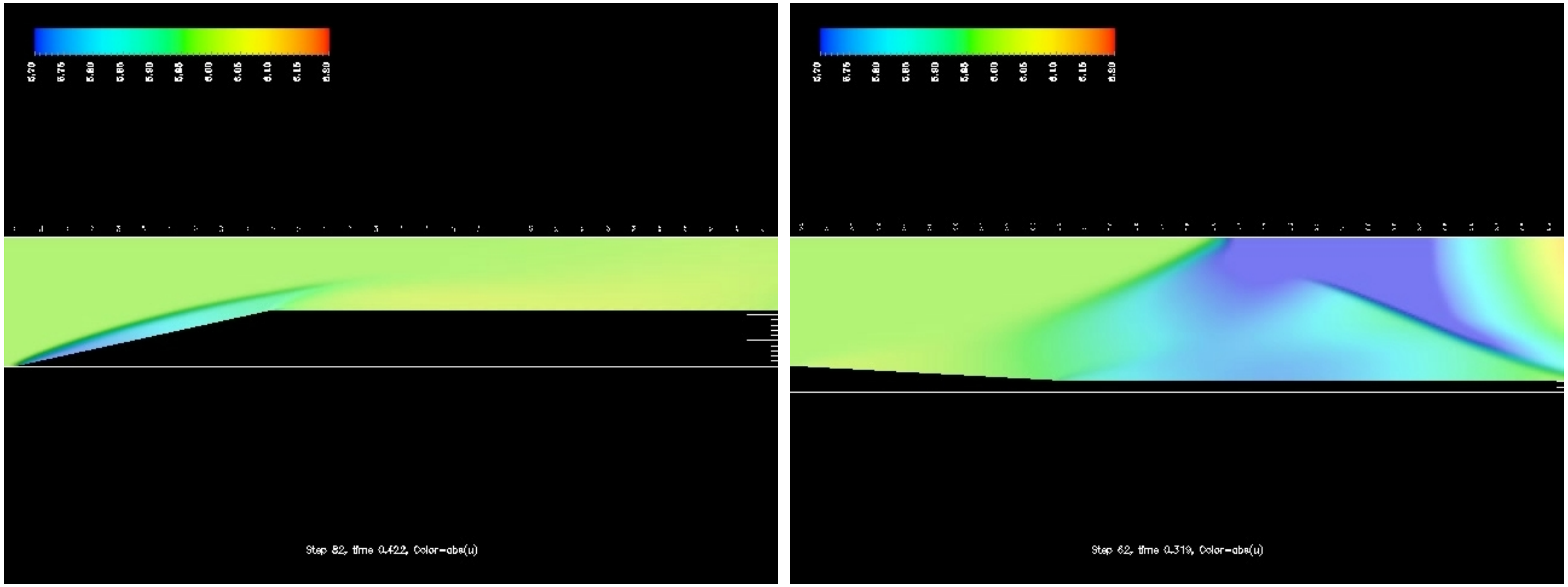

Elastically coupled ramp at Mach 6 (cont.)

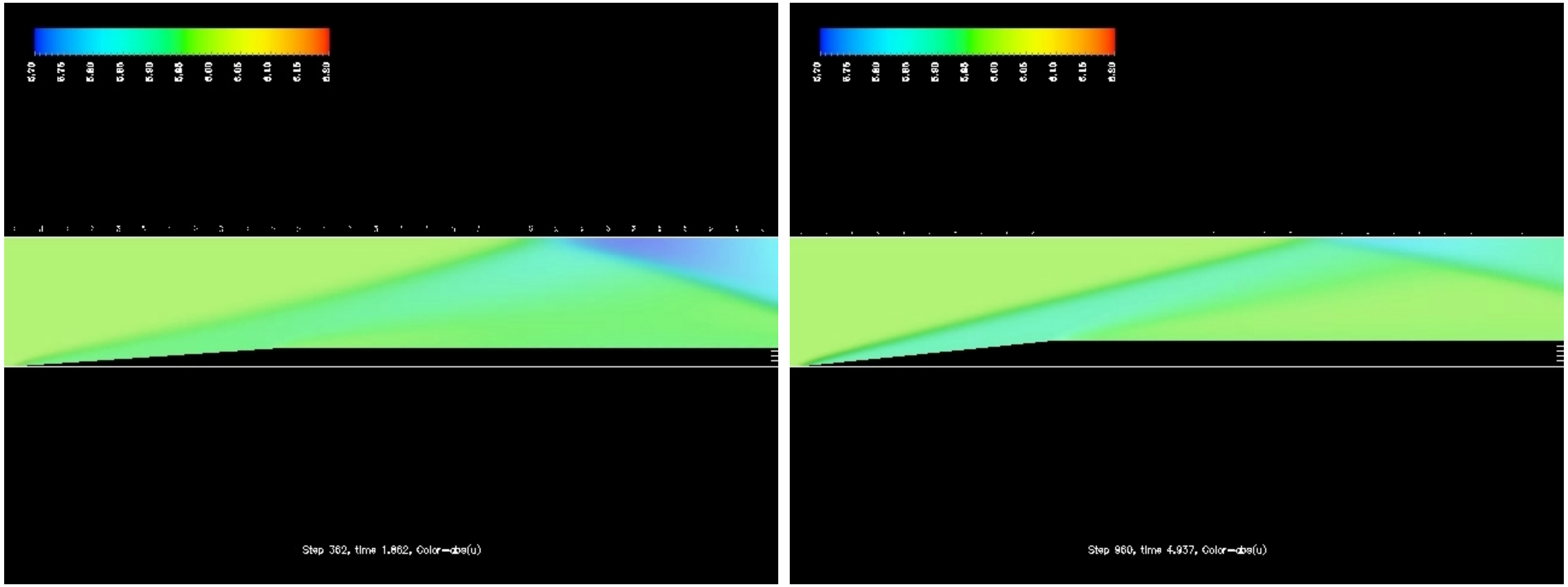

Acknowledgment

This work has received financial support from Consejo Nacional de Investigaciones Científicas y Técnicas (CONICET, Argentina, grants PIP 0198/98, PIP 02552/00, PIP 5271/05), Universidad Nacional del Litoral (UNL, Argentina, grants CAI+D 2000/43) and Agencia Nacional de Promoción Científica y Tecnológica (ANPCyT, Argentina, grants PICT 6973/99, PID-74/99, PICT Lambda 12-14573/2003, PME 209/2003).

We made extensive use of *Free Software* (`http://www.gnu.org`) as GNU/Linux OS, MPI, GNU-Guile, Python, PETSc, GCC/G++ compilers, Octave, Open-DX among many others. In addition, many ideas from these packages have been inspiring to us.